Using PMU Measurements to Assess Dynamic Line Rating of Transmission Lines

M.Sc. Thesis in
Electrical Power Systems and High Voltage Engineering

Sveinn Rúnar Júlíusson
Board of Studies of Energy
Aalborg University

AALBORG UNIVERSITY
DENMARK
STUDENT REPORT

Title:	Using PMU Measurements to Assess Dynamic Line Rating of Transmission Lines
Semester:	10th
Project period:	4/2 – 4/6 2013
ECTS:	30
Supervisor:	Claus Leth-Bak
Project group:	EPSH4-1032

Sveinn Rúnar Júlíusson

SYNOPSIS:

In this report a dynamic line rating(DLR) model is constructed. The overhead line which is subject of this report is the BR1 connection which is positioned in south west Iceland. The model uses measurements from a phasor measurement unit where from the impedance and admittance of a transmission line is computed. The impedance and admittance are acquired assuming the line can be modelled as a π-model. A numerical solver is constructed in order to compute the average height of the conductor using the information about the susceptance from the PMU measurements. The curve of a overhead line can be described by the catenary equation which is a hyperbolic function containing information about horizontal tension, weight per meter of the conductor and the span length. The horizontal tension decreases with increased conductor temperature and that relationship is there fore linearised while the weight per meter is kept constant. The span length varies through out the BR1 connection accordingly. The model is tested by implementing data from a fixative example where the result indicate that the equations are implemented correctly. The model is then tested in a case study using data from the BR1 connection. The result from the case study indicate that the model is not working properly. A sensitivity analysis is there fore conducted on the model, proofing that the model is very sensitive to any variation in the current angle. At last the model is tested by implementing the data of the BR1 connection in the simulation program DigSilent Powerfactory. By varying the load and the resistance the value of the susceptance deviates insignificantly. The model is there fore considered to work properly in theory but as the value of the susceptance is very sensitive to any variation in the current angle the model is not considered to be the ideal tool for DLR.

Copies: 3
Last page: 77
Last appendix: C

Summary

As the energy demand in the world is constantly increasing the utilisation of the existing transmission grids have to be maximised. The objective of this project is to construct a model which will utilise measurements from a phasor measurement unit (PMU) for dynamic line rating (DLR).
In Chapter 2 the BR1 connection is presented which is a 220 kV, 59 km overhead line which will be the subject of the DLR model. In the following chapters the theory of DLR, susceptance, Maxwell's potential, the catenary equation and the energy balance equation will be presented.
One of the limiting factors for transmitting electrical energy through overhead power line is the clearance of the conductor to the ground. As the load of the line is increased the current flowing through the line increases accordingly, thus resulting in increased conductor temperature. As the conductor lengthens the clearance to the ground reduces and as the conductor clearance gets closer to the minimum clearance the loading of the line approaches the capacity of the line. In order to determine the clearance of the conductor the value of the susceptance will be used. The value of the susceptance depends on the dimensions of the conductor. The susceptance can be computed by the Maxwell's potential coefficients, as described in Chapter 5.
In Chapter 6 the catenary equation is presented and the relationship between the overhead line and the catenary is described. The catenary variables are the horizontal tension, weight per meter and the span lenght. The variables of the catenary equation are varied in order to see how the result of the equation deviates.
In Chapter 7 the energy balance equation is presented and derived in order to acquire the conductor temperature.
The problem analysis part of this project is closed by the problem statement which introduces the problem to be examined, limitations of the project and which method to be used when solving the problem.
The model is constructed in Chapter 9 according to a flowchart which is presented in the beginning of the chapter. The model is constructed and tested by implementing a fixative example. The model proofs to work accordingly and the equations there fore implemented correctly.
In Chapter 10 a case study is performed using actual measurements from PMUs at each end of the BR1 connection and conducting measurements of the clearance at three different locations. The model results proof to be unrealistic and the measured clearance not according to the model results. The conductor temperature estimation by using the PMU measurements, comparing the measured value of the resistance to a reference value does not result in a realistic value of the conductor temperature and the estimation using the weather parameters and loading there fore used for that purpose. In Chapter 11 the input parameters to the model are varied in order to examine the effects of possible measuring error. The result of the variation indicates that the variation of the current angle has large effect on the susceptance value and variation of the voltage has large effect on the resistance value.
In Chapter 12 a simulation of the BR1 connection is performed using the simulation program DigSilent Powerfactory where the load is varied as well as the resistance of the conductor. The result shows that

the value of the susceptance does not depend on the loading nor the resistance in theory. However these factors do have impact on the susceptance as both the increased loading and increased resistance results in higher conductor temperature. As the calculation of the susceptance is done from the dimensions of the conductor and these dimensions do not change in the simulation as they do in reality. The conclusion of the project is that the dynamic line rating model based on the measurements from the phasor measurement unit is not affective in praxis due to sensitivity in the current angle measurements.

Preface

This report is written by Sveinn Rúnar Júlíusson on 10^{th} semester at Aalborg University - Board of Studies of Energy. The report is aimed at students in electrical power systems and high voltage engineering education.
The report is written in LaTeX. This report uses SI based units, derived units and prefixes as described by The International System of Units together with units outside of the SI standard. Sources are inserted using the Vancouver method, with a [number], which refers to the bibliography in the back of the report. Appendixes are declared with an A in front of the page number and can be found in the back of the report.
Additionally, a CD has been made, which features the report, sources and all programming in digital format.

A special thanks to Magni Þór Pálsson at Landsnet for professional discussions and help through out the project period. Also thanks to Hallgrímur Halldórsson at Landsnet for helpful information at final stages of the project period. I thank Verkís and VJI consulting for providing me with facility for working on the thesis through out the project period. Eymundur Sigurðsson and Ólöf Helgadóttir at VJI consulting for professional discussions through out the project period. And at last I would like to thank my supervisor, professor Claus Leth-Bak for professional discussions and valuable informations.

Table of contents

1 Introduction

In this chapter the motivation and background for the project will be introduced.

The electricity demand in the world is increasing and further utilisation of the existing transmission grids is there fore an important factor. A transmission line is usually designed to withstand load under a predefined conditions. These conditions are set to be in the save region and the rating of the transmission line is there fore higher then the actual operation load of the line. One of the limiting factors of a transmission line is the thermal limit. Increase in heat of the transmission line entails expansion to the conductor and there fore a decrease in clearance to the ground due to sag of the conductor.[1]
As mentioned the design of any transmission line is for a predefined condition and the transmission line has there fore certain rating of which the transmission line can transmit electrical energy. This rating can vary as the predefined conditions rarely apply. These predefined conditions or the external factors have a vital role in the rating of a transmission line. These factors are wind velocity, wind direction, air temperature and solar radiation. All these factors have impact on the conductor temperature which is the limiting factor when the rating is evaluated. In Iceland the evolution is the same as for the rest of the world as the energy production is gradually increasing while parts of the existing transmission system are kept unaltered.

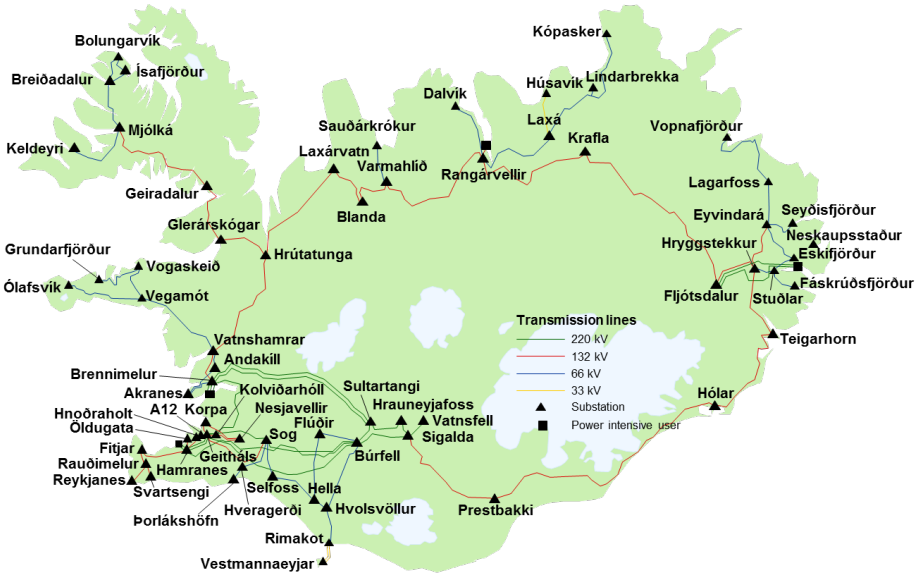

Figure 1.1: The Icelandic Transmission System [2]

In Figure 1.1 the Icelandic transmission system can be seen. In the south-west part of Iceland, which is the most populated area of Iceland, many large and small consumers are positioned, there fore the density of substations is very high in that area. A large number of transmission lines connect these substations to the power plants located in the surrounding area.

The substation at Brennimelur supplies two large energy consumers, Norðurál and Elkem. Norðurál and Elkem are positioned in the industry area at Grundartangi. Combined the two companies demand 620 MW or 5400 GWh per year.

Figure 1.2: The industry area at Grundartangi.

The substation Brennimelur is connected to various power plants by four connections. VA1 which is 100 MVA connection to northern Iceland(Blanda 150 MW).[3] SU1 and SU3 which are 470 MVA and 940 MVA respectively and connects the substation to the hydro power plants near Búrfell(Búrfell 270 MW, Hrauneyjafoss 210 MW, Sigalda 150 MW, Sultartangi 120 MW, and Vatnsfell 90 MW).[3] The fourth connection is BR1 which is a 304 MVA connection to the south and connects various geothermal power plants(Hellisheiði 303 MW, Nesjavellir 120 MW, Reykjanesvirkjun 100 MW and Svartsengi 75 MW) to the substation at Brennimelur.[4][5]
The BR1 connection is the most critical connection to the substation at Brennimelur as it is the lowest rated connection of the 220 kV lines. If the SU3 connection trips, the BR1 connection is prone to overloading according to given rating of BR1. At each end of the line BR1 is a phasor measurement unit(PMU) which measures both angle and magnitude of the currents and voltages. Along the BR1 connection are measuring points where the air temperature is measured as well as the wind velocity and direction.

The purpose of this project is to construct a dynamic model which will use the measurements of the PMU combined with weather measurements to assess the line sag and there from estimate the line rating.

2 System Description

In this chapter the transmission system of interest will be outlined and the relevant parameters listed.

The BR1 connection is a 220 kV connection which starts at the substation Geithals and lies through valleys and over mountains and sea towards the substation at Brennimelur as can be seen on Figure 2.1.

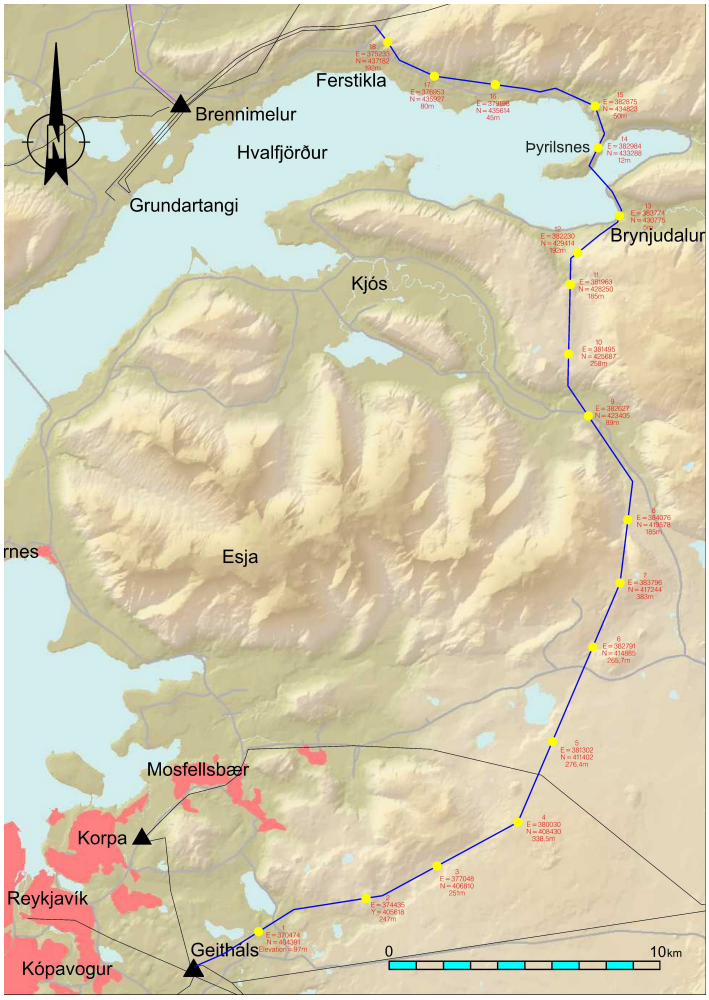

Figure 2.1: The layout of the BR1 connection. [2]

The transmission line is constructed with two types of conductors. The majority of the transmission line is of type All Aluminium Alloy Conductor(AAAC) 28.14 mm but where the sea is crossed the type

Aluminium Alloy Conductor Steel Reinforced(AACSR) 32.28 mm is used. The length of which the sea is crossed is around one kilometre where the total length of the transmission line is 59 km. The data for these conductors can be seen in Table 2.1.

		AAAC 28.14 mm	AACSR 32.28 mm
Number of wires	st	37	51
Size (Al/St)	mm	4.02/-	4.02/3.00
Area	mm^2	469.8/-	469.0/134.3
Tensile strength	MPa	57000	87000
Thermal expansion	10^{-6} °C	23	18
Weight	N/m	12.68	23.75
Diameter	mm	28.14	32.28
Breaking load	kN	131.2	294.3

Table 2.1: The data for the two different conductor types used in the BR1 connection.[6]

There are different types of masts used in the BR1 connection as the route of the transmission line is in valleys, over mountains and over sea. Depending on the circumstances the different types of masts are chosen. The different types can be seen in Figure 2.2.

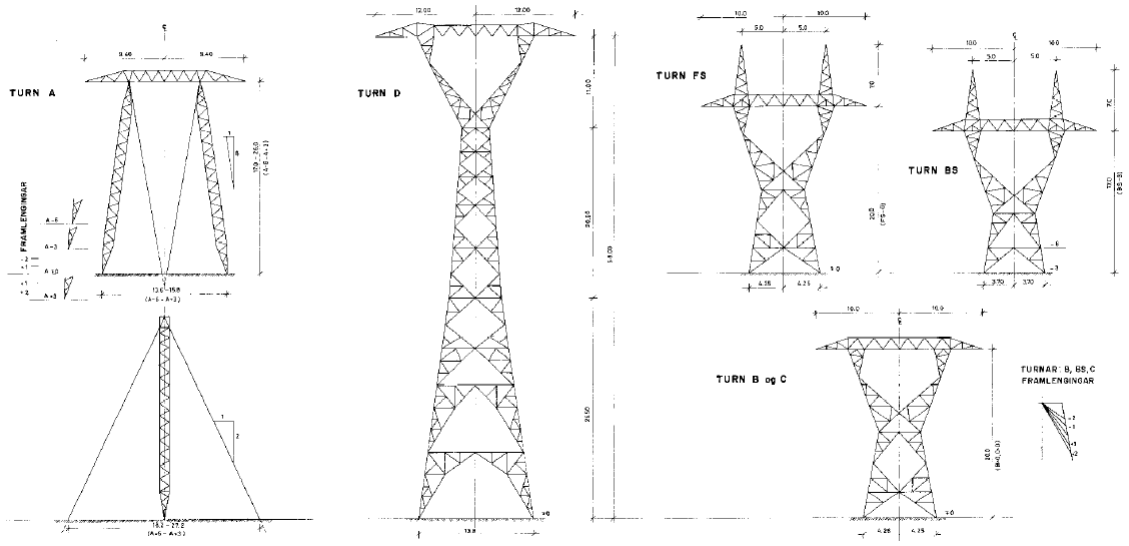

Figure 2.2: The types of masts used in the BR1 connection. [6]

The majority of the masts are of type "TURN A" seen furthest to the left in Figure 2.2. The rating of the BR1 connection is 304 MVA which is computed according to so called standard conditions which are wind of 0.6 m/s perpendicular to the conductor, ambient air temperature of 10℃ and effect of the solar radiation is neglected. The conductor temperature at the standard conditions and full load is 40℃.

I PROBLEM ANALYSIS

3 Dynamic Line Rating (DLR)

In this chapter the concept of Dynamic Line Rating(DLR) will be introduced and the method of how DLR can be useful for Transmission System Operators(TSO).

Static or fixed rating of a transmission line has been used by system operators in order to ensure the conductor does not sag below a specified limit. This specified limit is set to prevent contact with objects such as trees, houses, vehicles etc. thus affecting the reliability of the transmission and the safety of all living things. When transmitting energy through a transmission line the conductor gets hotter due to the current flow and the ohmic resistance of the conductor. As the conductor gets warmer it also expands which results in an increase in the sag of the conductor. The transmission line is there fore not to be exposed to loading that exceeds this rating in order to maintain a secure clearance between the conductor and the ground.
Comparing the capability of a transmission line using static line rating and DLR the following Figure 3.1 demonstrates the difference.

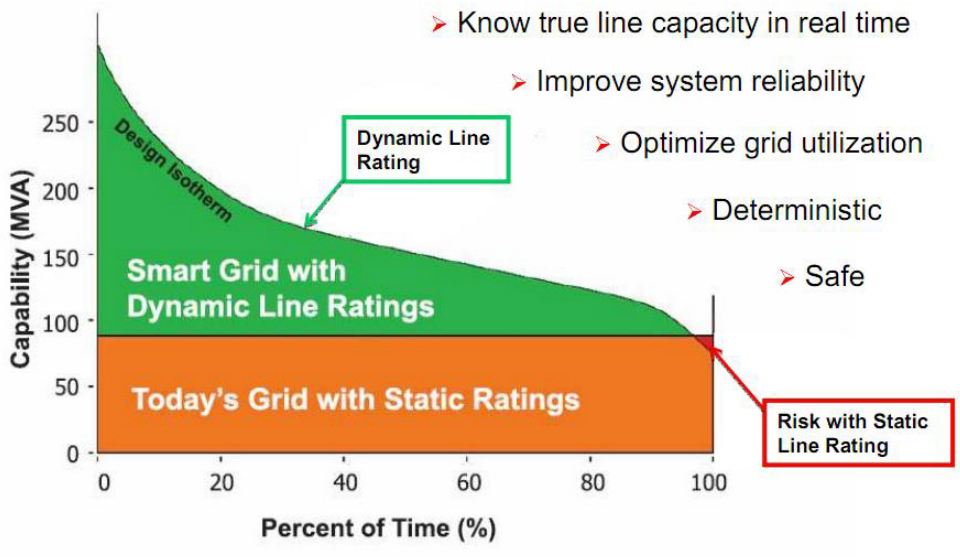

Figure 3.1: Demonstration of the improvements in utilisation of the transmission line using DLR.[7]

By applying DLR the risk that is resulted while using the static line rating will be avoided and the utilisation of the transmission line can improve in more than 90% of the time of operation.

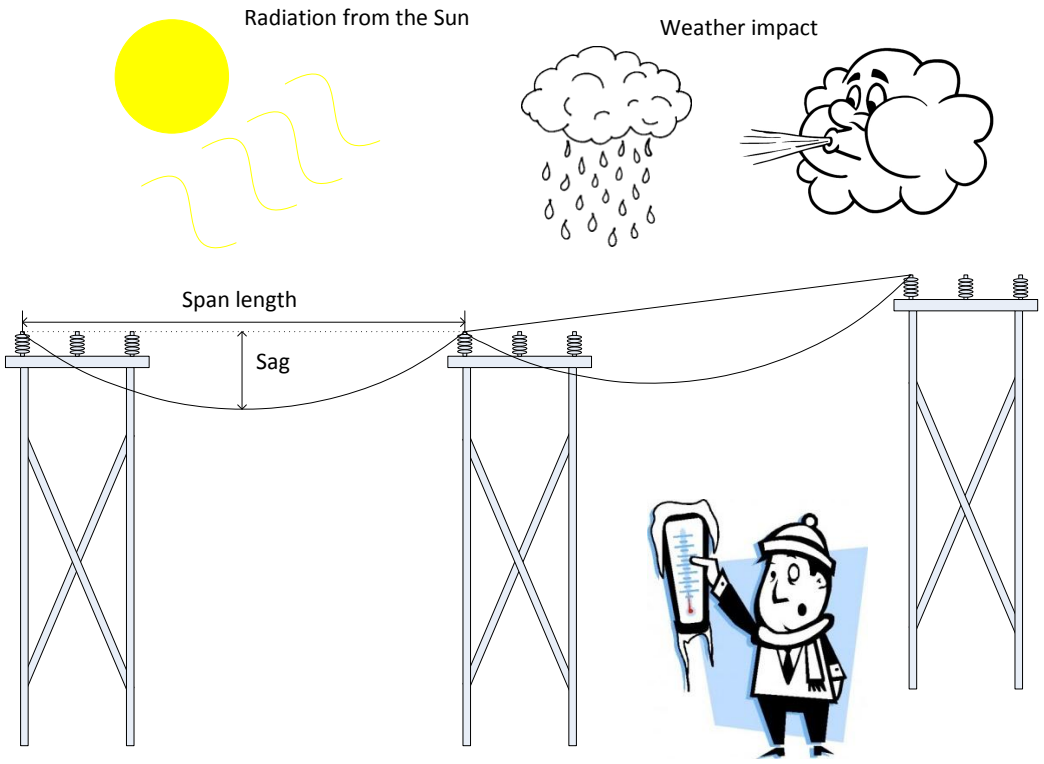

Figure 3.2: The sag of the conductor depends on external factors such as weather conditions.

DLR is the rating of a transmission line or section at the present time where the present condition are the deciding factors, identifying the ampacity in real time. Static Line Rating is on the other hand the rating of a transmission line under predefined conditions which represents the worst case scenario regarding the cooling of the conductor.
DLR can there fore be used to increase the loading of transmission lines according to the weather condition as the conductor will not sag as much while exposed to cold windy weather compared to calm hot weather. By applying DLR, existing transmission lines can be utilised further without investing in change of the structures or replacement of the conductor. The deciding factors for DLR are external factor which either cool down or warm up the conductor. The Sun radiation will warm up the conductor while the wind cools down the conductor. Surrounding temperature also has impact s on the conductors temperature. In Iceland the temperature tends to be lower compared to the mainland of Europe. When comparing the monthly average temperatures in Iceland, Denmark and Italy as can be seen in Figure 3.3 the difference of average temperature is around 12℃ between Iceland and Italy during the summer months.

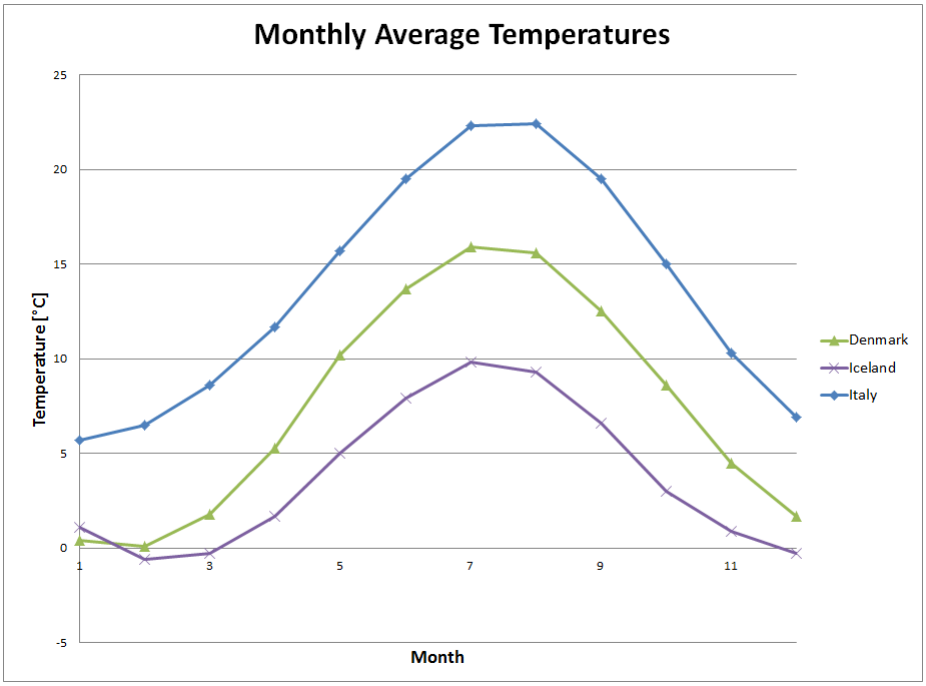

Figure 3.3: Monthly average temperature in Iceland, Denmark and Italy.[8]

The difference in temperatures can result in an increase in capacity for the same type of transmission line in Iceland compared to countries with higher average temperatures.

4 Phasor Measurement Unit (PMU)

In this chapter the Phasor Measurement Unit(PMU) will be described and it's function will be outlined.

PMU is a device which measures the electrical waves of an electrical system such as transmission line.

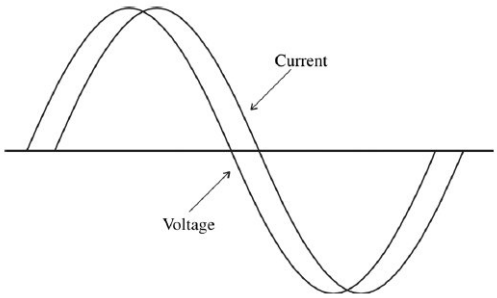

Figure 4.1: Waveform of current and voltage with small difference in angle.

These waves are so called phasors which are represented by an angle and a magnitude. By implementing a PMU to both ends of a transmission line the state of the line can be monitored. The impedance of the transmission line can be detected by comparing the values of the phasors at each end of the transmission line. By comparing the effect loss the resistance can be computed and by comparing the angles the reactive part can be computed, thus the impedance by combining these two parts.
The PMU can be a specialised device which only serves as PMU or it can be combined with the protection.

Figure 4.2: The PMU unit positioned at Geitháls.

At Brennimelur and Geitháls the PMU is of type SEL-487E which is a Transformer Differential Relay - Three Phase Transformer Protection Automation, and Control System. The SEL-487E is currently only used as a PMU unit but is designed as protection. The SEL-487E provides differential protection, earth fault protection, harmonic blocking, overcurrent protection and more. The SEL-487E can be used as a station-wide synchrophasor measurement device (Phasor Measurement(PMU)) and has 24 analog channels for that purpose. The SEL-487E can measure the voltage and current phase angles and is a useful tool for stability studies and load angle measurements.[9] The PMU performs measurements 50 times per second and each measurement has a time stamp. The accuracy of the time associated to each measurement is extremely important in order of comparing to the measurement at the other end of the transmission line. For this purpose the SEL-2401 clock is connected to the PMU unit. The clock is connected to SEL-9321 voltage supply. The SEL-2401 and SEL-9321 can be seen in Figure 4.3.

Figure 4.3: The clock for the PMU unit.

The SEL-2401 clock uses a GPS signal for determining the time accurately. In Figure 4.4 the antenna which acquires the GPS signal and is connected to the SEL-2401 clock can be seen.

Figure 4.4: The GPS antenna

In Iceland several PMUs have been installed. In Figure 4.5 their locations can be seen as the green diamonds.

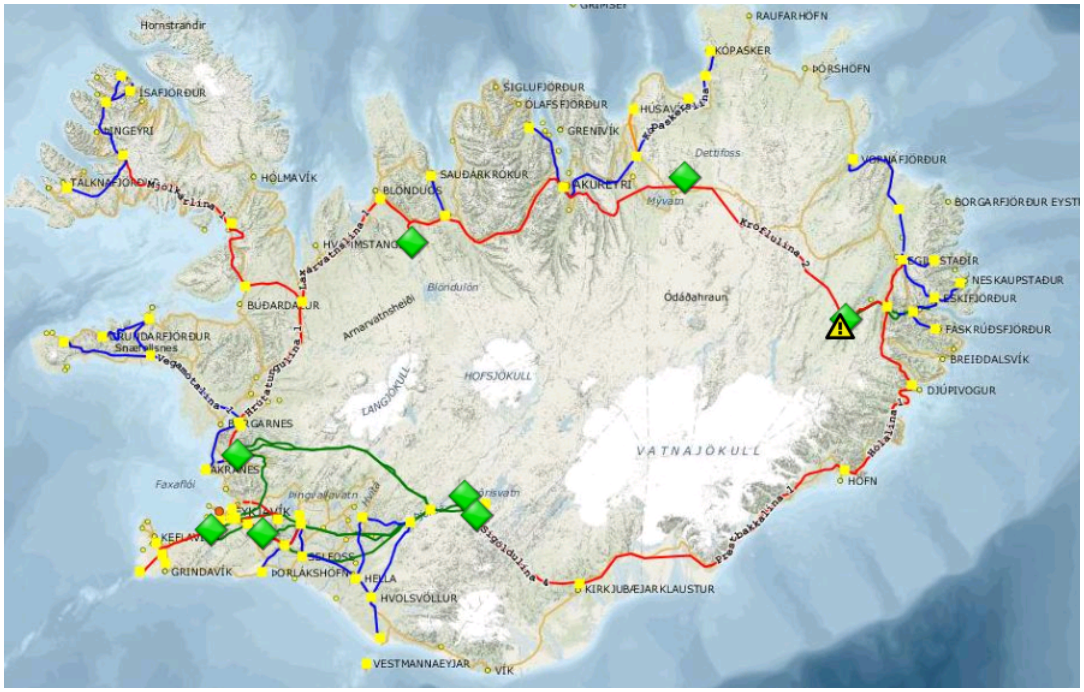

Figure 4.5: The PMU locations in Iceland.[2]

Currently the PMUs at Landsnet are only used for monitoring the system, WAMS (wide-area monitoring system). The future plans of Landsnet is to use the PMUs for automated control, WACS (wide-area controlling system).

5 Susceptance and Maxwell's Potential

In this chapter the concept susceptance will be introduced and the method of how the value of the susceptance can be acquired from PMU measurements. The Maxwell's potential coefficient will also be introduced and how it relates to the susceptance.

5.1 Susceptance

Susceptance(B) is the imaginary part of the admittance(Y) which is the inverse of the impedance(Z).

$$Y = \frac{1}{Z} \quad [\text{S}]$$

Admittance is measured in siemens, S, which is the inverse of Ω. The value of the admittance is a complex number where the real part is the conductance, G, and the imaginary part, B, is the susceptance as earlier mentioned.

$$Y = G + jB \quad [\text{S}] \quad (5.1)$$

Susceptance is also in linear relation with the capacitance and the frequency

$$B = \omega C = 2\pi f C \quad [\text{S}] \quad (5.2)$$

In order to compute the impedance and admittance of a transmission line a model is constructed. For modelling the transmission lines a two port network as shown in the following Figure 5.1 is useful. V_S and I_S represent the sending end voltage and current and V_R and I_R represent the receiving end voltage and current.

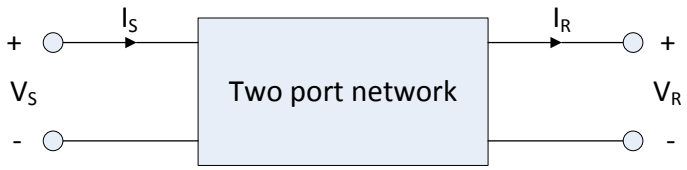

Figure 5.1: Two port network.

For short lines, 80 km or shorter and if the voltage does not exceed 69 kV, a series impedance circuit is sufficient when for modelling the transmission line. For longer lines, 80-250 km, a nominal π-model

is more useful as it includes the shunt capacitance.[10] In a nominal π circuit model the parameters are considered lumped where half of the shunt admittance is associated with each end of the transmission line. For transmission lines longer than 250 km an equivalent π-circuit model is used, where the parameters are considered distributed along the transmission line. Other methods for modelling transmission lines exist but are not considered here. When constructing a transmission line model the two port network shown in Figure 5.1 can be replaced by one of the following models shown in Figures 5.2 and 5.3.[11]

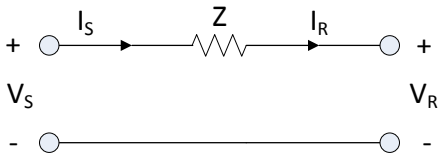

Figure 5.2: Series impedance circuit model.

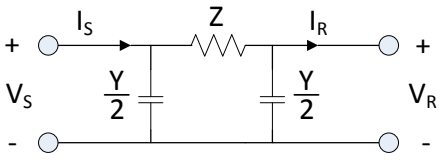

Figure 5.3: π circuit model.

In the nominal and equivalent π-models the same model circuit is used as the difference lies in the parameter determination. The relation between the sending end and receiving end of the transmission line can be written in matrix form using the so called ABCD parameters. These parameters depend on the resistance, R, inductance, L, conductance, C, and susceptance, G. The following equation describes the relation between the ABCD parameters and the sending and receiving end voltages and currents.[11]

$$\begin{bmatrix} V_S \\ I_S \end{bmatrix} = \left[\begin{array}{c|c} A & B \\ \hline C & D \end{array}\right] \begin{bmatrix} V_R \\ I_R \end{bmatrix}$$

As is mentioned in Chapter 2 the transmission line is 59 km long and there fore the short line approximation would be satisfying for modelling the transmission line, but as the voltage level is 220 kV the nominal π model is to be used as the shunt capacitance cannot be ignored. For the nominal π model the ABCD matrix becomes as following:[11]

$$\left[\begin{array}{c|c} 1+\frac{YZ}{2} & Z \\ \hline Y\left(1+\frac{YZ}{4}\right) & 1+\frac{YZ}{2} \end{array}\right] \tag{5.3}$$

As mentioned in Chapter 1 the purpose of this project is to construct a dynamic model using the measurements from the PMU. From the PMU the sending and receiving end voltages and currents are acquired. From this measurements the impedance and admittance, the ABCD parameters can be found by solving the following equations.

$$V_S = \left(1+\frac{YZ}{2}\right)V_R + ZI_R \quad [\text{V}] \tag{5.4}$$

$$I_S = Y\left(1+\frac{YZ}{4}\right)V_R + \left(1+\frac{YZ}{2}\right)I_R \quad [\text{A}] \tag{5.5}$$

$$Y = \frac{2(I_S - I_R)}{V_S + V_R} \quad [\text{S}] \tag{5.6}$$

$$Z = \frac{V_S^2 - V_R^2}{V_S I_R + V_R I_S} \quad [\Omega] \tag{5.7}$$

From the admittance the operation capacitance can be computed as shown in Equations 5.1 and 5.2. The operational capacitance is also known as positive and negative sequence capacitance.

5.2 Maxwell's potential coefficient

The potential of a conductor, where the effect of charges from the conductor own charge and other conductors charges is counted for, is computed by the following equation.

$$V_i|_{i=1,\ldots,N} = \sum_{j=1}^{N} P_{ij} Q_j \quad \text{[V]} \quad (5.8)$$

P_{ij} is the Maxwell's potential coefficient and Q_j is the charge. This method is based on the assumption that the conductors are infinitely long and perfectly horizontal above earth. In practise the conductors are however not perfectly horizontal above earth, they are strung between two masts forming a curve. The self-potential coefficients are the same for all the conductors given that they all are the same size and their clearance to the ground is the same. The following equation shows how the self-potential coefficient is calculated.

$$P_{ii} = 17.975109 \cdot log_e\left(\frac{2y_i}{r_i}\right) \quad \text{[km/}\mu\text{F]} \quad (5.9)$$

Where the y_i is the average height of the conductor above the ground, the clearance to the ground. y_i is multiplied by two because the value represents the distance to the electrostatic image of the conductor. r_i is the radius of the conductor or the conductor bundle in case of more than one conductor is strung for each phase. For the mutual-potential coefficient the following equation is computed.

$$P_{ij} = 17.975109 \cdot log_e\left(\frac{D_{ij}}{d_{ij}}\right) \quad \text{[km/}\mu\text{F]} \quad (5.10)$$

D_{ij} is the distance from conductor i to the electrostatic image of conductor j as can be seen in Figure 5.4. d_{ij} is the distance between the conductors i and j.

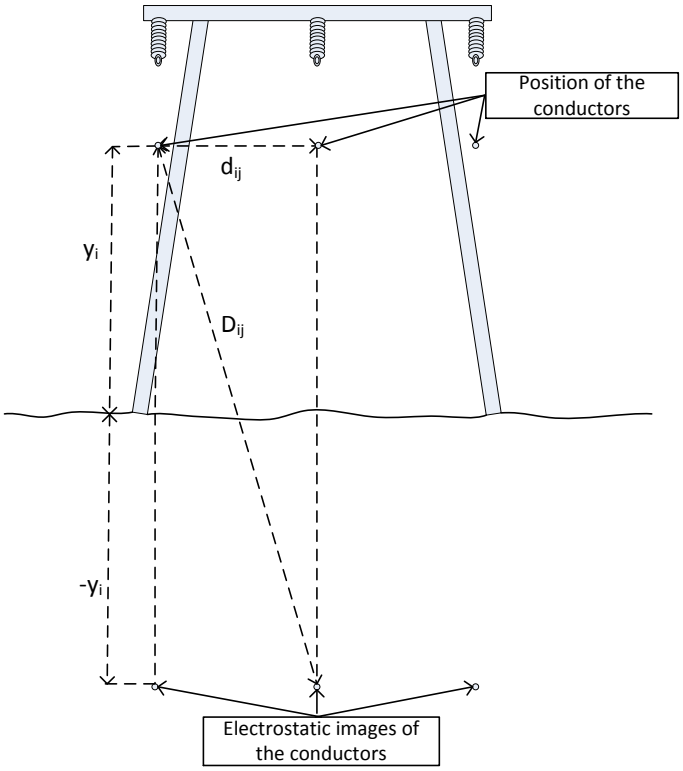

Figure 5.4: Dimensions of the parameters used to calculate the Maxwell's potential coefficient.

In Figure 5.4 the parameters mentioned in Equations 5.9 and 5.10 can be seen. The positioning of the conductors in Figure 5.4 is not at the attachments due to line sag and the height y_i represents the average height of the conductor.

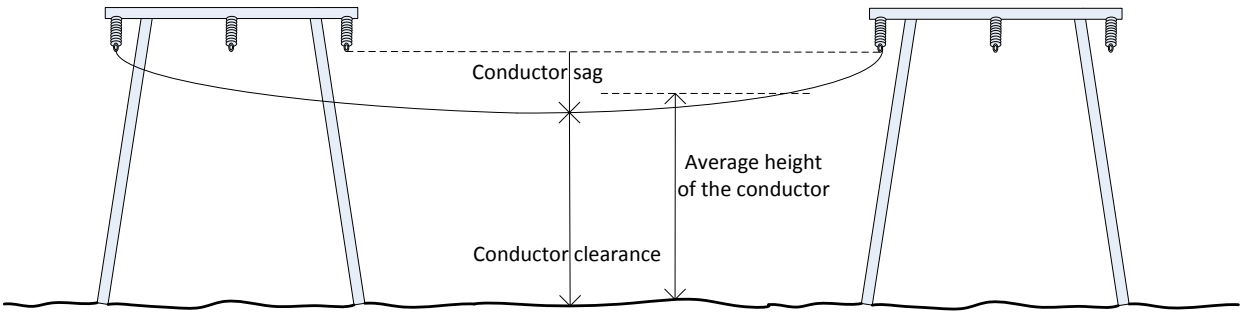

Figure 5.5:

After computing all the potential coefficients the values are arranged in a N x N matrix respectively. The size of the matrix depends on number of conductors or conductor bundles. For three phases without earth wires the matrix is a 3 x 3.
Rewriting the Equation 5.8 a relation between the potential matrix and the capacitance matrix is found,

resulting in the following.

$$\mathbf{C} = \mathbf{P}^{-1} \quad [\mu\text{F/km}] \tag{5.11}$$

The susceptance matrix, **B** is then constructed by multiplying the capacitance matrix with ω according to Equation 5.2. The sequence susceptance matrix is computed according to the following equation.

$$\mathbf{B}^{PNZ} = \mathbf{H}^{-1}\mathbf{B}\mathbf{H} \tag{5.12}$$

Where **H** equals the following.

$$\mathbf{H} = \begin{bmatrix} 1 & 1 & 1 \\ h^2 & h & 1 \\ h & h^2 & 1 \end{bmatrix}$$

Where $h = e^{j2\pi/3}$.
This shows the connection between the susceptance computed from the nominal π-model and the $\mathbf{B}^{PNZ}$, the sequence matrix which can be used to acquire the average height of the conductor.
From the average height of the conductor the average sag can be computed by solving the following equation numerically.

$$H_{av} = \frac{\sqrt{(2H_t - S_{av})S_{av}}}{\log_e\left(\frac{H_t + \sqrt{(2H_t - S_{av})S_{av}}}{H_t - S_{av}}\right)} \quad [\text{m}] \tag{5.13}$$

Where the H_{av} is the average height, H_t is the height of the mast and S_{av} is the average sag of the conductor.[12]

6 The Catenary

In this chapter the equation of the catenary will be introduced and the relevance to the modelling of a transmission line.

James Bernoulli(1654-1705) and John Bernoulli(1667-1748) known as the Bernoulli brothers who were from Basel in Switzerland. The Bernoulli brothers where mathematicians and known for several entries in the *Dictionary of Scientific Biography*. Among their work was showing that the following differential Equation 6.1 satisfies the shape of a hanging cable also known as the catenary.

$$a\frac{d^2y}{dx^2} = \sqrt{1+\left(\frac{dy}{dx}\right)^2} \tag{6.1}$$

a = T/ρ where T is the tension of the cable and ρ is the density of the cable. The Bernoulli brothers solved the differential equation showing that the shape of the hanging cable can be described by the following hyperbolic function:[13]

$$y = a\ \cosh\left(\frac{x}{a}\right) \tag{6.2}$$

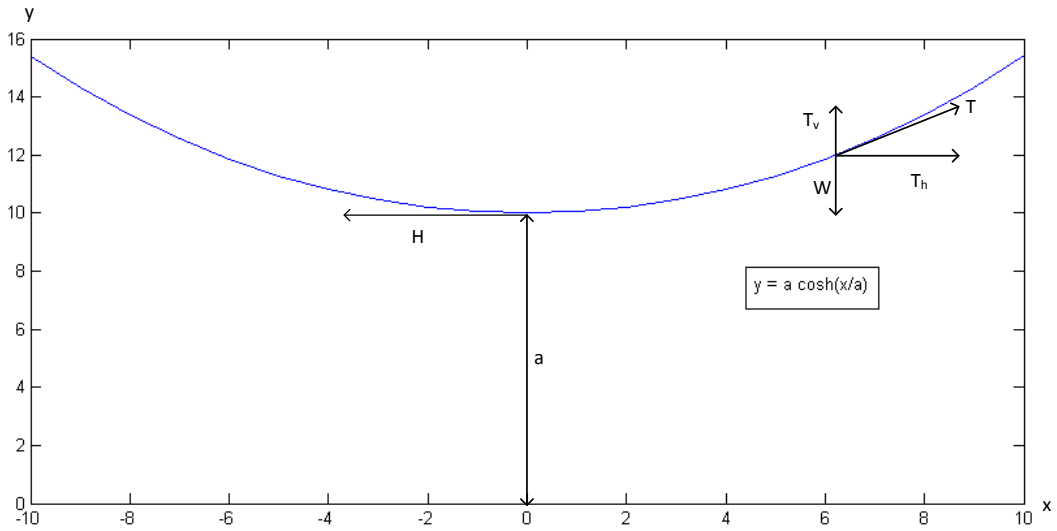

Figure 6.1: A catenary curve.

As can be seen in Figure 6.1 the x-axis variables are varied from -10 to 10 where the lowest point of the catenary is where x = 0. When looking at a span length the lowest point of the catenary is the midpoint of the span. By computing the Equation 6.2 where x is the midspan length and replacing the constant a

with $\frac{H}{W}$, the result shows the height of the attachments of the cable.

$$h = \frac{H}{W}\cosh\left(\frac{WS}{2H}\right) \quad [\text{m}] \quad (6.3)$$

Where H is the horizontal tension, W is the weight per meter of the cable and S is the span length. As the height of the attachments equals

$$h = a + D \quad [\text{m}] \quad (6.4)$$

Where a is the clearance to the ground as well as the constant from the Bernoulli equation 6.2 and D is the sag of the cable. The line sag can be computed according to the following

$$D = \frac{H}{W}\cosh\left(\frac{WS}{2H}\right) - \frac{H}{W} \quad [\text{m}] \quad (6.5)$$

The length of the catenary can be found by using the same method:[14]

$$\frac{L}{2} = \frac{H}{W}\sinh\left(\frac{WS}{2H}\right) \Rightarrow L = \frac{2H}{W}\sinh\left(\frac{WS}{2H}\right) \quad [\text{m}] \quad (6.6)$$

Equations 6.5 and 6.6 can be used to examine the behaviour of the catenary equation which represents the behavior of the transmission overhead line. Changing the variables such as span length, horizontal tension and the weight distribution is done in order to explore the different aspects of the parameter variation. The data for the BR1 connection was presented in Chapter 2. The data necessary for the calculation, is the area of the conductor as the horizontal tension is measured in MPa and the unit of the horizontal tension in the catenary equation is Newtons. The conductor area is 469.8 mm^2. Weight per meter of the conductor, which changes as conductor length changes, is 12.68 N/m at standard conditions. The horizontal tension is constant but differs between different tension towers. By varying the horizontal tension of the overhead line, with 400 m span, from 50-100 MPa the conductor sags according Figure 6.2..

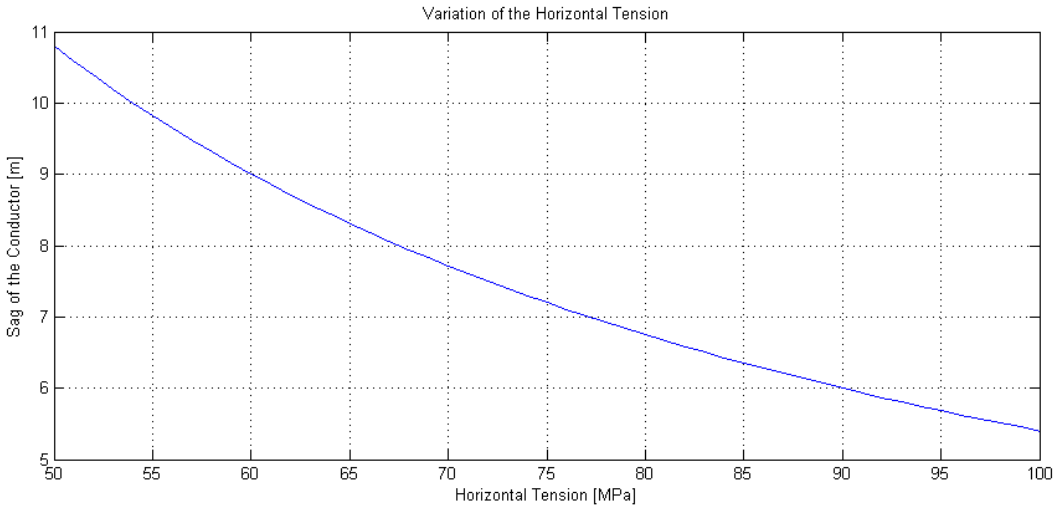

Figure 6.2: Variation of the horizontal tension.

From Figure 6.2 the impact of the horizontal tension is seen. The sag of the conductor differs from 10.8 m at 50 MPa to 5.4 m at 100 MPa.

The span lengths are not the same along the BR1 connection. By varying the span length and horizontal tension the variation of the sag can be seen in Figure 6.3.

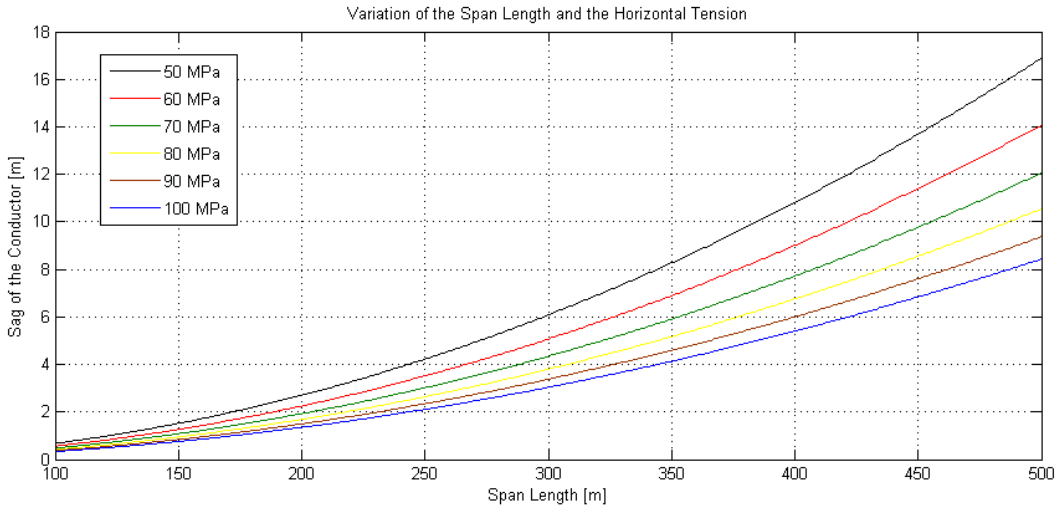

Figure 6.3: Variation of the span length and the horizontal tension.

As seen on Figure 6.3 the span length has large effect on the sag of the conductor also the effect of higher horizontal tension decreases the sag of the conductor.
As the conductor gets warmer, due to loading and external effects, it lengthens and there fore the weight per meter changes accordingly. In Figure 6.4 the weight per meter is varied from 5 N/m to 20 N/m.

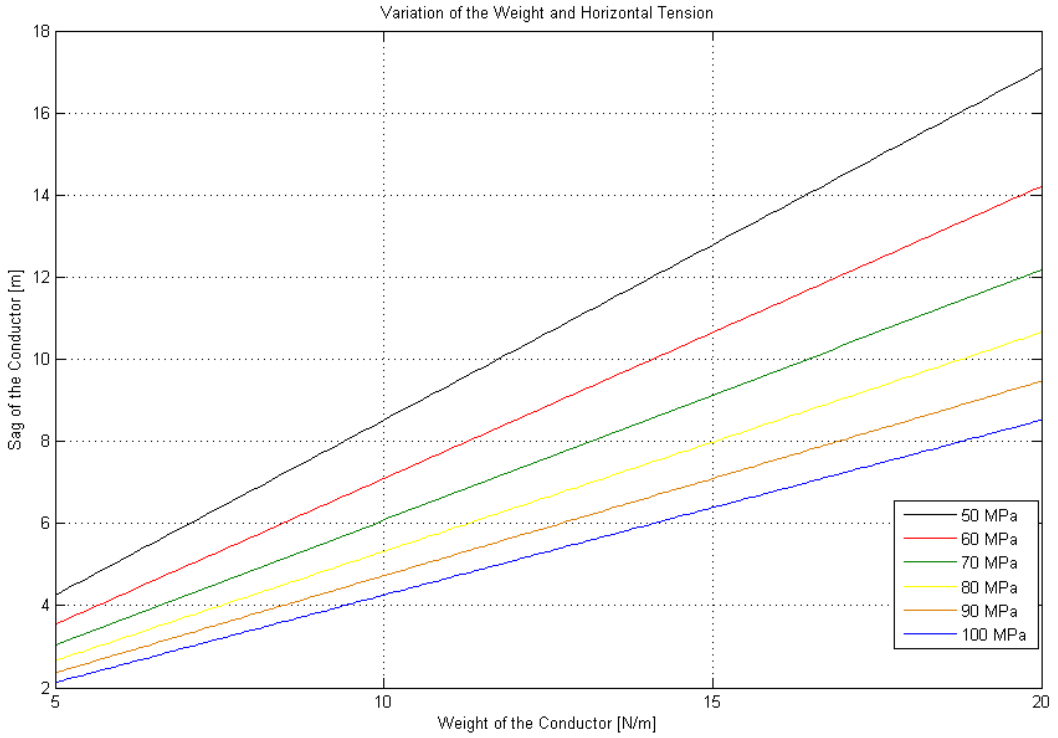

Figure 6.4: Variation of the weight of the conductor compared to different horizontal tension.

The weight per meter is not expected to change as much as Figure 6.4 demonstrates. As the conductor lengthens, the weight per meter will decrease which will according to the figure results in less sag of the conductor. In Figure 6.5 the weight per meter is varied in order to see the change of the length of the conductor.

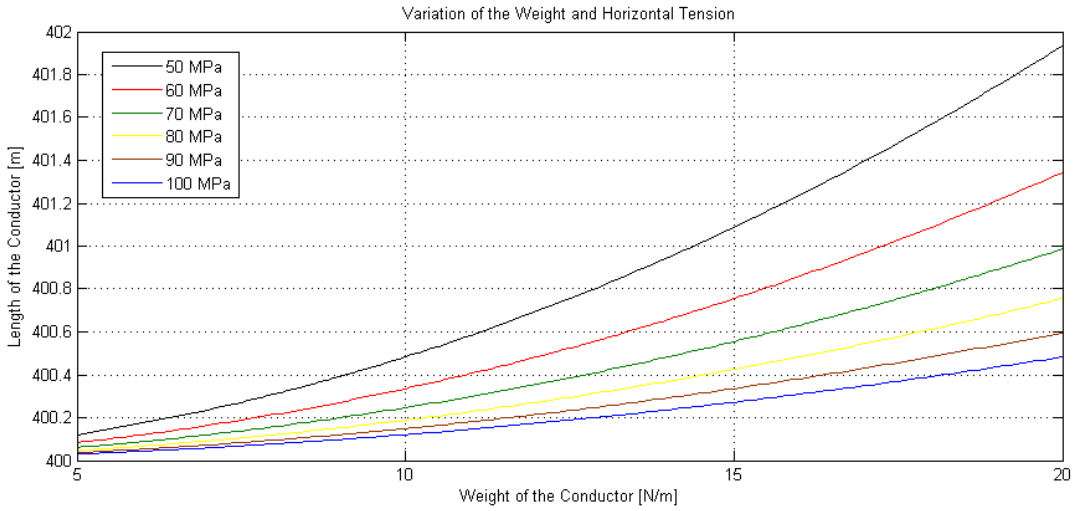

Figure 6.5: Variation of the weight of the conductor compared to different horizontal tension.

Varying the weight per meter and comparing the length of the conductor with the sag can be seen in Figure 6.6.

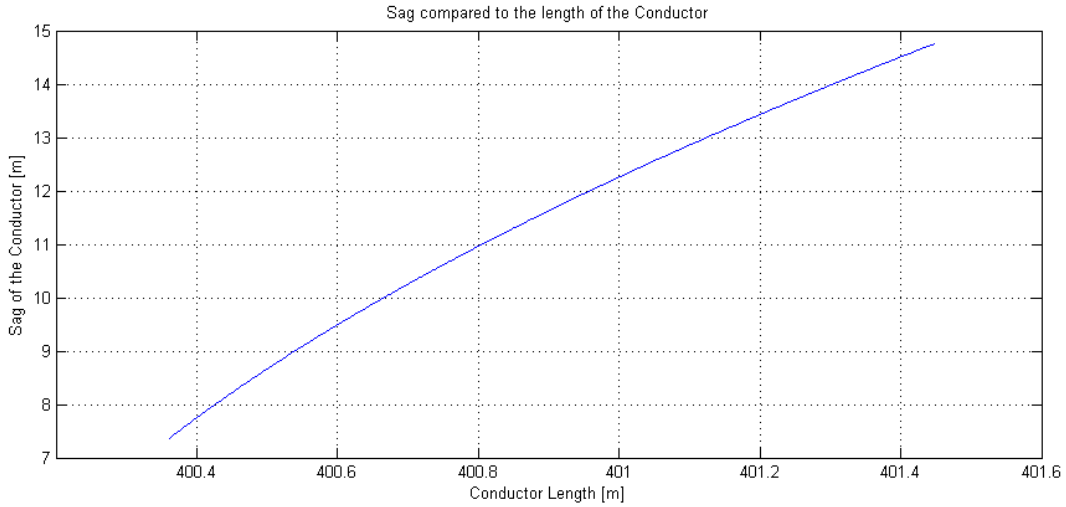

Figure 6.6: Variation of the conductor length compared to sag of the conductor.

As the variables of the catenary equation have been varied, the relation between the sag of the conductor and the weight per meter, tension and span length shows that by increase in span length the sag increases and by increasing the tension the sag decreases. As the conductor lengthens the weight per meter will decrease. According to the variation of the weight per meter the sag decreases as the weight per meter decreases. The total weight of the conductor between two masts can not decrease and the

sag of the conductor will there fore not decrease from the change of the weight per meter. From Figure 6.6 it is clear that the sag does increase, but will not increase linearly.

7 Energy Balance Equation

This chapter introduces the concept of energy balance and the relevance of energy balance to Dynamic Line Rating of a transmission line. Further more will the energy balance equation be derived according to references [15] and [16].

Energy balance equation is another way of introducing the conservation of energy which is a version of the first law of thermodynamics which states that "energy can be neither created nor destroyed during a process; it can only change forms."[17] While there is no work done by a system all energy entering a system must be equal to the energy leaving the system. As a transmission line transmits electrical energy and certain amount of the energy is "lost" because of the resistance of the conductor. When the transmission line is a subject to a change in energy transportation there is however a certain amount of work done which results in a storage of energy within the conductor. The largest contributor is the energy refereed to as ohmic losses, which heats up the conductor. The radiation from the sun also has the affect of heating the conductor but is minor compared to the ohmic losses. These two factors are said to inject heat energy to "the system". While the conductor is hotter than the atmospheric air around it, the conductor heats up the air by radiation, by radiation the conductor looses heat energy to the surroundings. When there is wind there is also a convection which cools down the conductor. The following Equation 7.1 shows this relationship.[15]

$$Q_{stored} = Q_{\Omega} + Q_S - Q_R - Q_C \quad \text{[W/m]} \quad (7.1)$$

Where

Q_{stored} is the energy stored by the conductor

Q_{Ω} is the conductor losses(Heating the conductor)

Q_S is the radiation from the sun(Heating the conductor)

Q_R is the radiation from the conductor(Cooling the conductor)

Q_C is the convection e.g. cooling from the wind

The main purpose of using this equation is to compute the conductor temperature and in order to proceed a certain assumptions has to be made. The conductor is considered to be isothermal for an average temperature. The AC resistance is considered to be linear, which is reasonable up to temperatures of 150℃, the conductors are not expected to reach such temperatures.
For radiation terms for the energy balance equation, only direct solar energy is considered. From these assumptions made, the energy per unit length is:

$$Q_{stored} = mc_p \frac{dT}{dt} \quad \text{[W/m]} \quad (7.2)$$

Where m is the mass per unit length and c_p is the specific heat constant(c_p for aluminium is 954 $J/kg°C$). T is the temperature and t is the time. As mentioned earlier the AC resistance is linearised as the following equation demonstrates.

$$I^2 R_{AC} = I^2(A + BT) \quad (7.3)$$

A is the AC resistance at 0℃ and B is a temperature coefficient which describes how the resistance changes with temperature. The absorption of the solar energy can be described by following equation:

$$Q_S = D\epsilon_s Q'_s \quad \text{[W/m]} \quad (7.4)$$

D is the conductor diameter, ϵ_s is the absorptivity of the conductor and Q'_s is the solar energy per unit area. The convective heat transfer is:

$$Q_C = \pi Dh(T - T_\infty) \quad \text{[W/m]} \quad (7.5)$$

Where h is the convective heat transfer coefficient and T_∞ is the air temperature. h is computed in terms of Nusselt number, Nu.

$$\text{Nu} = 0.53(\text{GrPr})^{1/4} \quad (7.6)$$

Where Gr is the Grashof number and Pr is the Prandtl number. For simplification the properties of air will be assumed constant and the following expression is derived:

$$h = \frac{k}{D} 10^{(2.217 + 0.652\log(VD) + 0.0355(\log(VD))^2)} \quad (7.7)$$

Where V is the wind speed. The convective heat constant in Equation 7.7 does however not include effect of wind direction, the following equation is there fore needed for correction.[18]

$$\frac{\text{Nu}(\omega)}{\text{Nu}(\omega = 0)} = 1.194 - \sin(\omega) - 0.194\cos(2\omega) + 0.368\sin(2\omega) \quad (7.8)$$

Where ω equals direction of the wind measured in radians. The radiative heat transfer is computed by following equation:

$$Q_R = \pi D\epsilon_i \sigma(T^4 - T_\infty^4) \quad \text{[W/m]} \quad (7.9)$$

Where ϵ_i is the emissivity, σ is the Stefan-Boltzmann constant (5.67×10^{-8} W/m^{2}K^4). The non-linear term $(T^4 - T_\infty^4)$ can be linearised by the following term.

$$(T^4 - T_\infty^4) = E(T - T_\infty) \quad (7.10)$$

Where $E = (1.38 + 0.0139T_\infty) \times 10^8$ [K^3].
Combining these equations into the original Equation 7.1 results in:

$$mc_p \frac{dT}{dt} = I^2(A + BT) + D\epsilon_s Q'_s - \pi D\epsilon_i \sigma E(T - T_\infty) - \pi Dh(T - T_\infty) \quad \text{[W/m]} \quad (7.11)$$

Solving Equation 7.11 for the conductor temperature results in:

$$T = T_\infty + \frac{I^2(A + BT_\infty) + \epsilon_s D Q_s'}{\pi h D + \epsilon_i \pi D \sigma E - I^2 B} \quad [^\circ C] \quad (7.12)$$

From Equation 7.12 the conductor temperature is computed where the effect of current, wind speed, wind direction and air temperature is included. Equation 7.12 can be used to calculate the conductor temperature under various loading conditions by changing the current value. As the load is increased on a transmission line the temperature of the conductor will increase according to the following equation.

$$T = T_1 e^{-t/t_c} + T_2(1 - e^{-t/t_c}) \quad [^\circ C] \quad (7.13)$$

Where T_1 and T_2 are the temperatures at the initial load and final load respectively. The t_c is the time constant and is computed as follows.[15]

$$t_c = \frac{m c_p}{\pi h D + \epsilon_i \pi D \sigma E - I_2^2 B} \quad [\text{min}]$$

Where I_2 is current at final load condition. Plotting the result using the data for the BR1 connection while increasing the load from 200 MVA to 350 MVA can be seen in following figure.

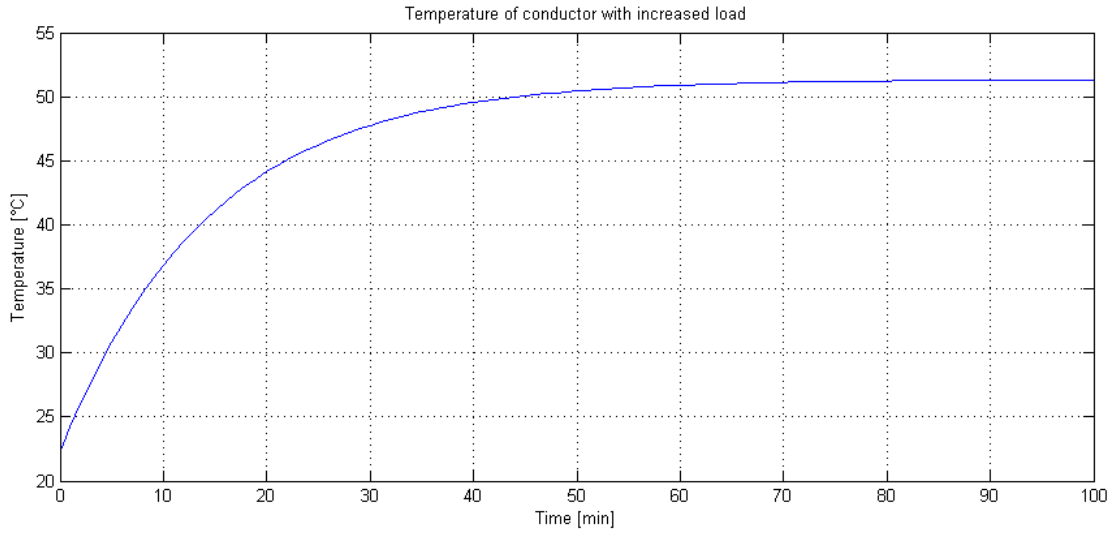

Figure 7.1: The transient behaviour of the conductor heat while exposed to increased loading.

It is clear from the figure that a sudden increase in load from 200 MVA to 350 MVA for short time, 10-20 minutes, will not have severe impact on the transmission line, resulting in a failure. The conductor temperature rises from 22℃ to 44℃ after 20 minutes. After 80 minutes the temperature has reached steady state which results in a conductor temperature of 51.31℃.

8 Problem Statement

Problem to be Examined

The purpose of this project is to use measurements from a Phasor Measurement Unit(PMU) and the weather measurements to determine the dynamic line rating of a transmission line. The transmission line will be modelled by constructing a MATLAB script.
A case study will be assembled in order to compare the results of the model with actual measurements.

Limitations

- A level span is presumed.
- The earth wires are neglected as they are only present close to the substations.
- The part of the transmission line where the sea is crossed is not considered to be a critical part.

Method

The transmission line will be modelled as a nominal π circuit where the parameters will be approximated by using the $ABCD$ parameters. A numerical solver will be constructed by computing the Maxwell's potential coefficient where the average height of the conductor is unknown parameter. The sequence susceptance will be computed from the numerical solver and compared to the actual value found from the $ABCD$ parameters. Further more additional weather measurements will be used to access the conductor temperature using the energy balance equation.

II PROBLEM SOLVING

9 Model

In this chapter the model will be constructed according the methods and equations presented in the problem analysis part of this report.

9.1 Model Design

The purpose of this project is as mentioned in the problem analysis to construct a model which uses measurements from a PMU for dynamic line rating of overhead transmission lines. For that purpose the flowchart in Figure 9.1 is constructed.

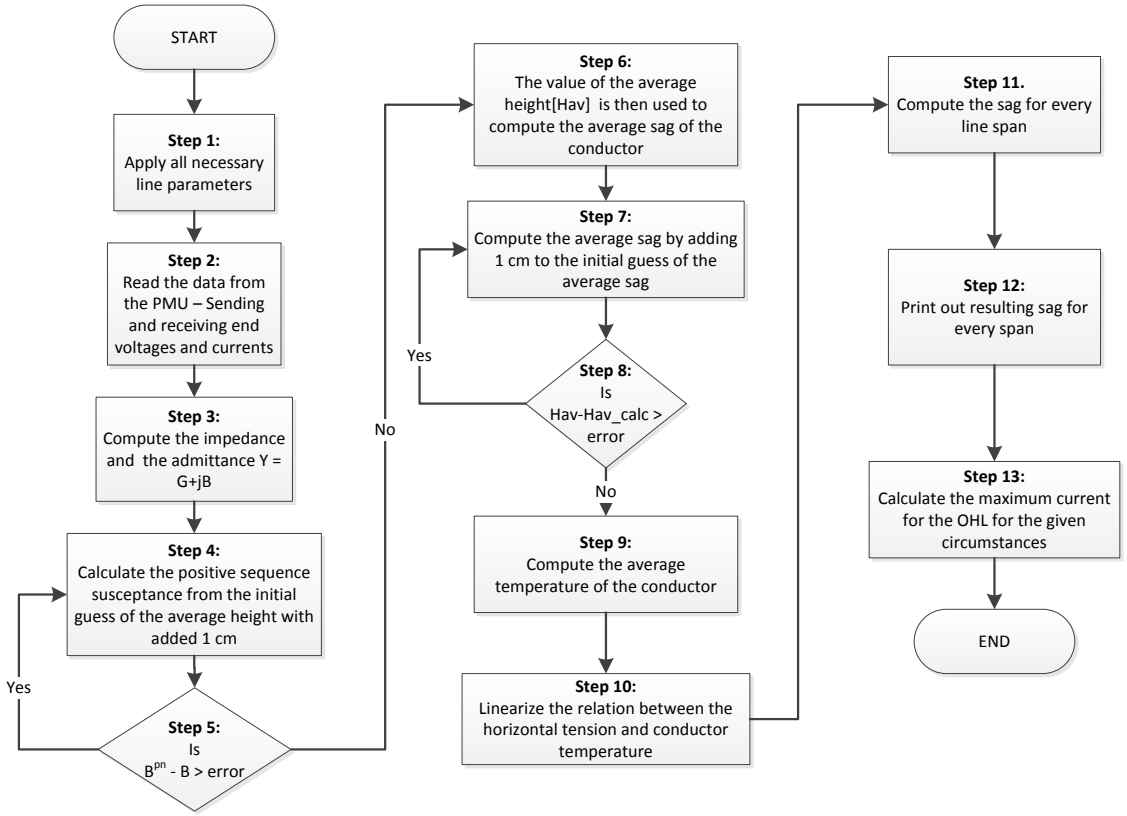

Figure 9.1: The flowchart for the model.

In **step 1** of the flowchart all parameters of the OHL are implemented into an m-file. These parameters are conductor area, conductor radius, distance between the phases, tensile strength of aluminium and thermal expansion coefficient of aluminium.
In **step 2** the data from the PMU, the voltage and current phasors are imported to the model.
In **step 3** the impedance and admittance of the transmission line is computed according to following equations which where presented in Chapter 5.

$$Y = \frac{2(I_S - I_R)}{V_S + V_R} \quad [\text{S}]$$

$$Z = \frac{V_S^2 - V_R^2}{V_S I_R + V_R I_S} \quad [\Omega]$$

In **steps 4 and 5** a numerical solver is constructed, using the method presented in Chapter 5, where the susceptance is calculated by guessing the average height of the conductor. The solver starts with a initial guess and adds 1 cm to the average height in each iteration. The susceptance is computed by using the Maxwell's potential coefficient described in Chapter 5. The solver compares the resulting susceptance with earlier calculated susceptance acquired from the admittance in the previous step. When the difference between the susceptance from the numerical solver and from the PMU calculation reach certain accuracy the numerical solver stops and returns a value of the average height of the conductor. For accessing the dynamic line rating of a OHL the conductor clearance is to be known as the distance between the conductor and the ground is the limiting factor. As can be seen in Figure 9.2 the average height of the conductor is not equal to the conductor clearance to the ground.

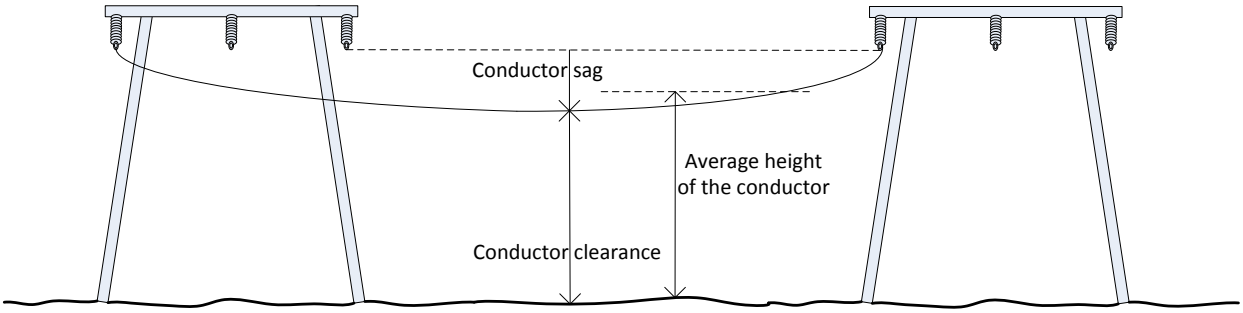

Figure 9.2: The average height, conductor clearance and the conductor sag in OHL.

In **steps 6, 7 and 8** a numerical solver is constructed in order to compute the conductor average sag the following equation which was described earlier in Chapter 5 is used.

$$H_{av} = \frac{\sqrt{(2H_t - S_{av})S_{av}}}{\log_e\left(\frac{H_t + \sqrt{(2H_t - S_{av})S_{av}}}{H_t - S_{av}}\right)} \quad [\text{m}]$$

The same procedure is used as in the previous numerical solver. The average sag is guessed until the resulting average height is the same as the average height computed in the previous step.
In **step 9** the average temperature of the conductor is calculated. The resistance of the conductor increases with temperature and knowing the resistance, the conductor temperature can be calculated by the following equation:

$$T = \left(\frac{R}{R_0} - 1\right)\left(\frac{1}{\alpha}\right) - T_0 \quad [^\circ C]$$

Where R_0 is the resistance at temperature T_0. R is the measured value of the resistance and α is the temperature coefficient of resistance.
The temperature can also be computed by using the method described in Chapter 7 using the following equation.

$$T = T_\infty + \frac{I^2(A + BT_\infty) + \epsilon_s D Q'_s}{\pi h D + \epsilon_i \pi D \sigma E - I^2 B} \quad [^\circ C]$$

In **step 10** the relation between the horizontal tension and temperature is linearised. As mentioned earlier the curve of the OHL can be described by the following hyperbolic function.

$$D = \frac{H}{W}\ \cosh\left(\frac{WS}{2H}\right) - \frac{H}{W} \quad [m]$$

The variables are horizontal tension H, weight per meter W and span length S. The horizontal tension is constant between two tension masts. As there are many tension masts in the BR1 connection the horizontal tension differs between the sections. When the conductor lengthens due to thermal elongation the horizontal tension decreases. In order to compute the combined thermal and elastic elongation of the conductor, the elongation of the conductor due to thermal effects is first calculated presuming a zero tension according to following two equations.[19]

$$ZTL_{ref} = L_{ref}\left(1 + \frac{H - H_{ref}}{EA}\right) \quad [m] \quad (9.1)$$

$$ZTL_{pres} = ZTL_{ref}\left(1 + \alpha\left(T_{pres} - T_{ref}\right)\right) \quad [m] \quad (9.2)$$

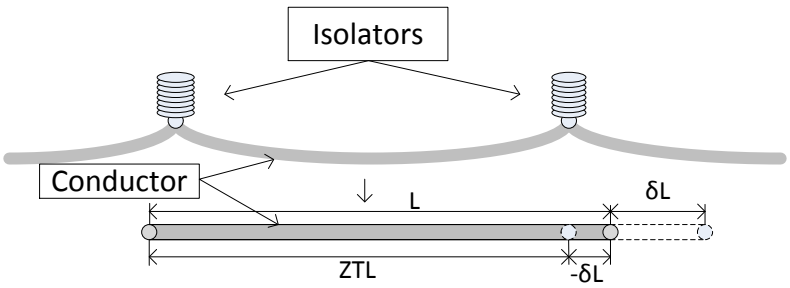

Figure 9.3: Zero tension length is shorter than the length of the cable when hanging from the masts.

ZTL is the length of the conductor if the conductor is taken down and laid on the ground with no tension. In Equation 9.1 ZTL_{ref} is the reference length of the conductor at 5℃. L_{ref} is the reference length of the conductor while strung to the mast at design conditions. H is set to zero and H_{ref} is the design horizontal tension. E is the modulus of elasticity of aluminium and A is the conductor cross sectional area.[19]

Next step is to calculate the length of the conductor when including the thermal elongation. ZTL_{pres} is the length of the conductor at present temperature. α is the thermal expansion coefficient, T_{pres} is the present temperature and T_{ref} is 5℃.
Next is to include the effect of the elastic elongation of the conductor. For that purpose an iterative process is needed where the following equations are used.

$$L_n = L_{(n-1)}\left(1 + \frac{H_{new} - H_{ref}}{EA}\right) \quad [\text{m}] \quad (9.3)$$

$$D_n = \sqrt{\frac{3S(L_n - S)}{8}} \quad [\text{m}] \quad (9.4)$$

$$H_n = \frac{WS^2}{8D_n} \quad [\text{N}] \quad (9.5)$$

Where n is the number of iteration. In Equation 9.3 the H_{new} is the value from the ZTL calculations in the first iteration but in the second iteration an average value for the ZTL and the first iteration is used according to following equation.

$$H_{new} = \frac{H_{(n-1)} + H_{(n-2)}}{2} \quad [\text{N}] \quad (9.6)$$

The iteration process is repeated 2-4 times and the results are plotted in x-y diagram. For the x-axis the elongation of the conductor is used and for the y-axis the horizontal tension is used. In the same graph the catenary equation is plotted using the same parameter where the elongation and horizontal tension is varied.[19] The location of intersection of the curves represents an equilibrium tension for each individual case. In Figure 9.4 the two curves have been plotted for the span length of 365 meters and conductor temperature of 50℃.

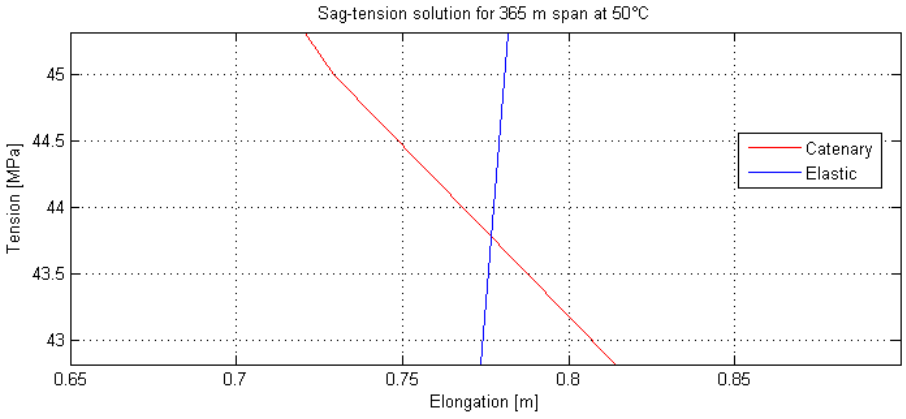

Figure 9.4:

By changing the conductor temperature the point of intersection changes. Gradually changing the conductor temperature and noting down the tension value at the intersection points results in a data set which is plotted and linearised as seen in Figure 9.5.

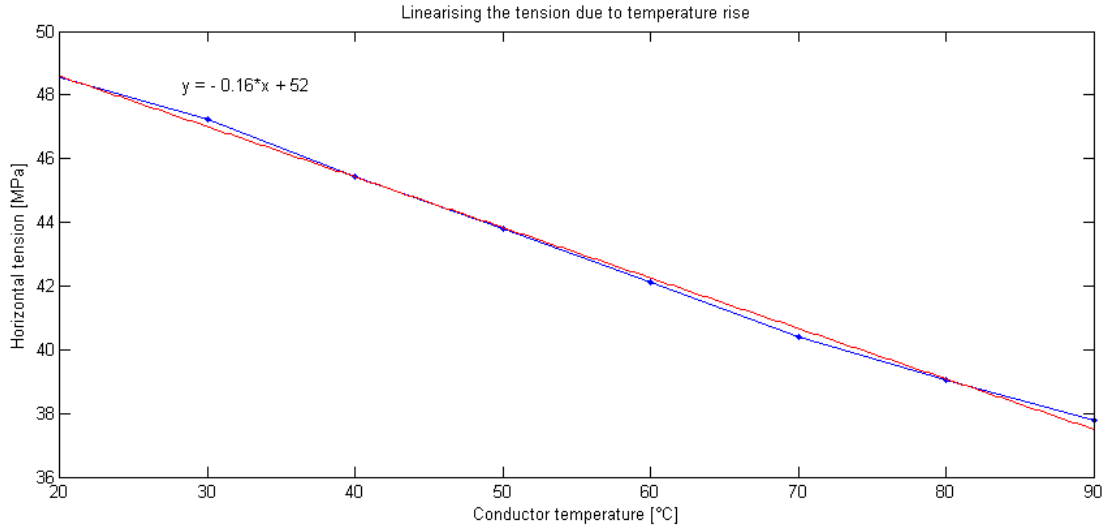

Figure 9.5: The point of intersection is deciding factor for the tension.

The section between the two tension masts, which where strung with 57.6 MPa at 5℃, can now be modelled using the approach for the horizontal tension resulting in the following equation.

$$H = -0.16T + 52 \quad \text{[MPa]} \quad (9.7)$$

Where T is the conductor temperature. Each section is calculated separately and the results can be seen in Appendix B.

The weight per meter, W [N/m] can differ when the conductor lengthens. In order to see how much W varies a following example is demonstrated.

For a 400 span, where the mast is 22 meters high and the minimum clearance to the ground is 7.4 meters the maximum sag is 14.6 meters which results in:

$$L = S + \frac{8D^2}{3S} \Rightarrow 400 + \frac{8 \cdot 14.6^2}{3 \cdot 400} = 401.42 \quad \text{[m]} \quad (9.8)$$

Computing the sag using the average horizontal tension and the weight per meter enlisted in Chapter 2 results in 9 meter sag. The length of the conductor when the sag is 9 meter is

$$L = 400 + \frac{8 \cdot 9^2}{3 \cdot 400} = 400.54 \quad \text{[m]} \quad (9.9)$$

The weight of the conductor is 12.68 N/m which equals 1.291 kg/m. The total weight in the 400 m span is then

$$400.54 \cdot 1.29 = 517.1 \quad \text{[kg]} \quad (9.10)$$

Considering the elongation of the conductor, the weight per meter changes to

$$\frac{517.1}{401.42} = 1.288 \quad \text{[kg/m]} \quad (9.11)$$

$$\Downarrow$$

$$1.288 \cdot 9.82 = 12.65 \quad \text{[N/m]} \quad (9.12)$$

The difference in the weight per meter is 0.03 N/m and when computing the sag of the conductor, according to the hyperbolic function, for the different values the difference is only 2 cm. There fore the effect of the variation of the weight per meter is neglected and W is there fore considered constant.

The span length, S, is a factor which can not change. The span length varies through out the BR1 connection as the landscape is not homogeneous.

The catenary equation will now be used for the modelling where the horizontal tension is linearised for each section of the BR1 connection. The model will there fore be different for each section.

$$D = \frac{aT+b}{W}\left(\cosh\left(\frac{WS}{2(aT+b)}\right)-1\right) \quad \text{[m]} \quad (9.13)$$

Where $aT+b$ represents the linearised horizontal tension where T is the average temperature of the conductor.
By reading in the data from Appendix A for the span lengths and mast heights, the sag is computed for every span. From these calculations the clearance is computed for every span and comparing the clearance with the minimum allowable clearance, 7.4 m.[20]

In **step 11** the transmission line is divided into sections, where each section is the route between one tension mast to another. As the tension is considered to be constant in every span between two tension masts. The model computes the sag of every span of each section with the tension calculated from previous step.
In **step 12** the results of the calculation from the previous step are printed out.
In **step 13** the maximum load is found by numerically solving Equation 7.12, from Chapter 7. The ampacity of the OHL can be determined by using the maximum conductor temperature and the weather parameters. If the weather parameters are unknown they can be predicted or a predefined condition can be assumed. The normal presumption Landsnet uses is 10℃, 0.6 m/s wind perpendicular to the OHL and zero radiation from the sun.[6]

9.2 Model Results

The data for the BR1 connection which was presented in Chapter 2 will be used for testing the model and the load of the transmission line will be estimated. This is done in order to see if the equations are implemented correctly within the model. The key parameters are as follows:

Power	MVA	304
Voltage (Sending end)	kV	$220 \angle 0°$
Resistance at 20℃	Ω/km	0.07279
Estimated conductor temperature	℃	40
Temperature coefficient of resistance	$℃^{-1}$	0.0036
Area of the conductor	mm^2	469.8
Weight of the conductor	N/m	12.68
Diameter of the conductor	mm	28.14

Table 9.1: The data for the fixative example.

The first step is to estimate the impedance of the line. The resistance is calculated according to following equation.

$$R = R_0 * [1 + \alpha(T - T_0)] \quad [\Omega/\text{km}] \quad (9.14)$$

Where R is the resistance at temperature, T and R_0 is the reference resistance at a reference temperature, T_0. α is the temperature coefficient of the resistance.
The reactance, X_L is computed as following equation demonstrates.

$$X_L = 0.0628\left(\ln\frac{D_M}{r} + \frac{1}{4}\right) \quad [\Omega] \quad (9.15)$$

D_M is the geometric mean distance and r is the conductor radius. Calculated according to the following equation.[21]

$$D_M = \sqrt[3]{D_{AB}D_{BC}D_{AC}} \quad [\text{m}] \quad (9.16)$$

Where D_{AB}, D_{BC} and D_{AC} is the distance between the phase conductors as seen in Figure 9.6.

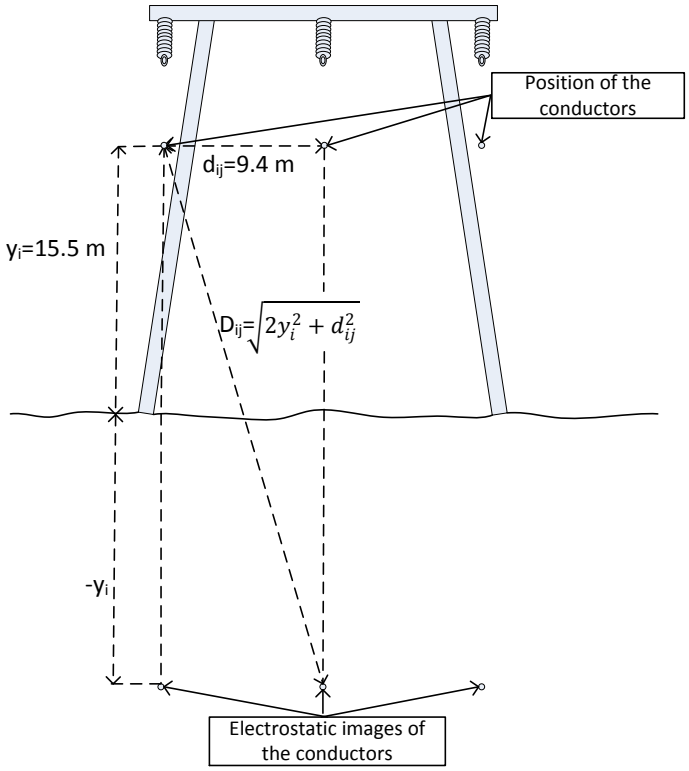

Figure 9.6: Dimensions used in the fixative example.

The resulting impedance for the conductor at a temperature of 40 ℃ is then.

$$R = 0.07279 \cdot [1 + 0.0036 \cdot (40 - 20)] = 0.0780 \ \Omega/\text{km}$$
$$D_M = \sqrt[3]{9.4 \cdot 9.4 \cdot 18.8} = 11.843 \ \text{m}$$
$$r_i = \sqrt{\frac{469.8 \cdot 10^{-6}}{\pi}} = 0.0122 \ \text{m}$$
$$X_L = 0.0628 \cdot \left(\ln \frac{11.843}{0.0122} + \frac{1}{4} \right) = 0.4475 \ \Omega/\text{km}$$
$$Z = R + jX_L = 0.078 + j0.4475 \ \Omega/\text{km}$$

The susceptance is computed as described in Chapter 5. As mentioned in Chapter 5 the average height of the conductor is needed in order to compute the Maxwell's potential coefficient. The average height of the conductor is there fore predefined as 15.5 m. The predefined value is also the expected output from the model. The potential matrix is computed according to Equations 5.9 and 5.10.

$$P_{ii} = 17.975109 \cdot log_e\left(\frac{2y_i}{r_i}\right) \quad [\text{km}/\mu\text{F}]$$

$$P_{ij} = 17.975109 \cdot log_e\left(\frac{D_{ij}}{d_{ij}}\right) \quad [\text{km}/\mu\text{F}]$$

$$P_{AA} = P_{BB} = P_{CC} = 17.975109 \cdot \ln\left(\frac{15.5}{0.0122}\right) = 140.85 \text{ km/}\mu\text{F}$$

$$P_{AB} = P_{BC} = 17975109 \cdot \ln\left(\frac{\sqrt{9.4^2 + (2 \cdot 15.5)^2}}{9.4}\right) = 22.21 \text{ km/}\mu\text{F}$$

$$P_{AC} = 17.975109 \cdot \ln\left(\frac{\sqrt{(2 \cdot 9.4)^2 + (2 \cdot 15.5)^2}}{(2 \cdot 9.4)}\right) = 11.78 \text{ km/}\mu\text{F}$$

The resulting potential matrix is:

$$\mathbf{P} = \begin{bmatrix} 140.85 & 22.21 & 11.78 \\ 22.21 & 140.85 & 22.21 \\ 11.78 & 22.21 & 140.85 \end{bmatrix} \quad [\text{km/}\mu\text{F}]$$

Where $\mathbf{C}_{phase} = \mathbf{P}^{-1}$ and $\mathbf{B}_{phase} = \omega \mathbf{C}_{phase}$.

$$\mathbf{B}_{phase} = \begin{bmatrix} 2.30 & -0.34 & -0.14 \\ -0.34 & 2.33 & -0.34 \\ -0.14 & -0.34 & 2.30 \end{bmatrix} \quad [\mu\text{F/km}]$$

Next is to transpose the phase quantities to PPS(positive phase sequence),NPS(negative phase sequence) and ZPS(zero phase sequence) using the h operator, $h = e^{j2\pi}$, with the **H** transformation matrix as mentioned in Chapter 5, Equation 5.13.
The resulting sequence matrix is:

$$\mathbf{B}_{PNZ} = \begin{bmatrix} 2.58 & -0.074 - j0.13 & 0.027 - j0.046 \\ -0.074 + j0.13 & 2.58 & 0.027 + j0.046 \\ 0.027 + j0.046 & 0.027 - j0.046 & 1.76 \end{bmatrix} \quad [\mu\text{F/km}]$$

As the BR1 connection is 59 km the resulting impedance and admittance is:

$$Z = 4.605 + j26.402 \quad [\Omega]$$

$$Y = j15.24 \quad [\mu\text{S}]$$

The sending end complex power is estimated to be 302.5+j30 MVA and the sending end voltage is estimated to be 220 kV at 0° angle as the sending end is assumed to be the reference point. The sending end current is acquired by computing $S = 3VI^* => I^* = \frac{S}{3V}$.
The receiving end voltage and current is acquired by solving the following equation earlier presented in Chapter 5.[11]

$$\begin{bmatrix} V_S \\ I_S \end{bmatrix} = \left[\begin{array}{c|c} 1 + \frac{YZ}{2} & Z \\ \hline Y\left(1 + \frac{YZ}{4}\right) & 1 + \frac{YZ}{2} \end{array}\right] \begin{bmatrix} V_R \\ I_R \end{bmatrix}$$

The expected data from the PMU is there fore as follows:

	Magnitude/angle
Sending end voltage	220 ∠ 0° kV
Sending end current	797.8 ∠ -5.66° A
Receiving end voltage	214.8 ∠ -5.48° kV
Receiving end current	800.1 ∠ -8.03° A

Table 9.2: Expected data from the PMU.

Running the model described in Chapter 9 results in a average height of 15.47 meters as the estimated height of the conductor was 15.5 meters the accuracy is:

$$Accuracy = \frac{15.47}{15.5} \cdot 100\ \% = 99.8\ \%$$

The model calculates the average height with good accuracy and the model is there fore considered to work accordingly and the equations implemented correctly.

9.3 Model Implementation

In order to make use of the model it has to be implemented to the TSOs monitoring system. In Figure 9.7 a simple network connection of PMU is demonstrated. As mentioned in Chapter 4 the PMUs are connected to each end of a transmission line. As the sampling frequency is relatively high the accuracy of the time stamp associated to each measurement is very important as the measurements are to be compared. A GPS antenna is there fore connected to the PMU in order of securing accurate time stamp. The PMUs are connected to WLAN through router and the data acquired from the PMUs is gathered in a server which is positioned in Landsnet's headquarters in Reykjavík. Landsnet's employees can access the data by logging on to the server through their workstation.

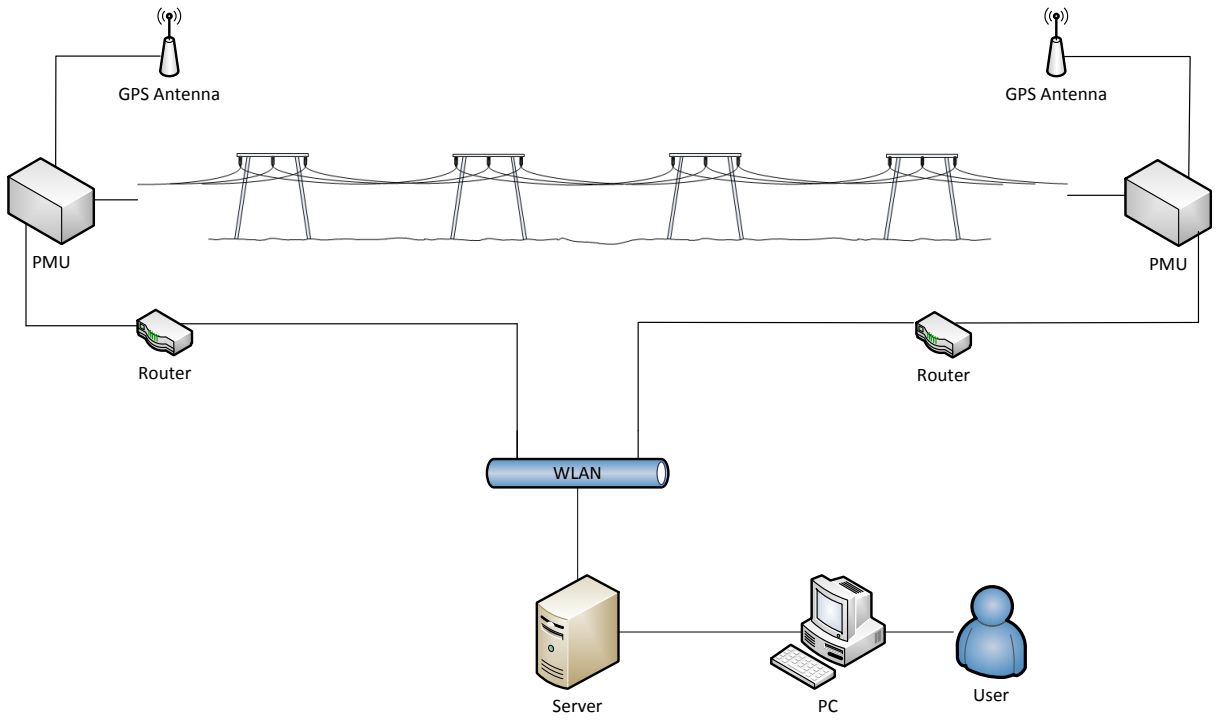

Figure 9.7: The PMU network connection.

The line rating can be computed for each measurement and the line rating there fore evaluated with the same frequency as the signal gathering. As the voltage and currents fluctuate constantly the resulting line rating would not give the correct picture. An average value of the DLR over a certain time, computing once every minute for 5-10 minutes would there fore give better picture of how the line rating is.

A computer program would be constructed which uses the model presented in Chapter 9. The program would have to be implemented into TSO's user interface in order to be visual to the system operators which are monitoring the system. If there is a sudden drop within the rating of the system an alarm should go of indicating possibility of overloading of the associated transmission line.
By implementing DLR to all transmission lines the security of electrical energy supply would increase, especially in warm and calm weather, and would respectively increase the utilisation of the system in cold and windy weather.

III

CASE STUDY

10 Case Study

10.1 Introduction to Case Study

In this chapter a case study is introduced where the model will be tested under different circumstances.

The reason for a case study is to test the model earlier described and constructed. The voltage and current magnitudes and angles from the PMUs will be applied to the model and the results of the model compared to actual measurements of the line sag. The sending and receiving end voltages and currents are compared and the impedance as well as the susceptance are calculated. The average temperature of the transmission line is calculated and the model is run accordingly as described in Chapter 9.
In order to test the model result the clearance of the conductor to the ground is measured. In order to measure the height of the transmission line a Suparule Cable Height Meter Model 300E, as seen in Figure 10.1, is used. The meter utilises ultrasonic signal to determine the height of the transmission line. The meter is positioned on the ground, directly under the transmission line. The meter transmits an ultrasonic signal towards the conductor and measures the time it takes the echo to return. The meter has a build in thermometer and automatically compensates for any variation caused by the air temperature.[22]

Figure 10.1: The distance meter for measuring the conductor height.

When conducting the measurement a spot is chosen by assuming the mid point of the span and then conduct number of measurements around that spot. The measurements are noted down and the lowest value considered to be the mid point of the span.

Figure 10.2: Span 16 of the BR1 connection

10.2 Measurements

Measurements where conducted at 17:00 on may 6th 2013. The load of the BR1 connection was 229.9 MVA and the output from the PMU was as enlisted in Table 10.1.

	Magnitude/angle
Sending end voltage	$222.7 \angle 168.03°$ kV
Sending end current	$596.13 \angle 157.27°$ A
Receiving end voltage	$215.5 \angle 161.28°$ kV
Receiving end current	$600.7 \angle 155.04°$ A

Table 10.1: The data from the PMU.

Three spans where selected with respect to accessibility. The clearance of the conductor was measured with the suparule height distance meter displayed in Figure 10.1 according to the method described in Section 10.1.

Span nr.	Measured Clearance				
11	11.17	10.95	**10.66**	10.68	10.74
16	11.01	10.82	10.40	**10.03**	10.38
17	21.11	**17.89**	18.43	20.09	18.03

Table 10.2: Height measurements of selected spans of the BR1 connection

The weather conditions at the measurement location was

	Value
Air temperature	5.6℃
Wind velocity	4.2 m/s
Wind angle	18°
Solar radiation	0 W/m^2

Table 10.3: The data from the weather station at the location.

10.3 Model results

The data acquired from the PMU unit was then implemented into the model constructed in Chapter 9. The result of the model is listed in the following table.

Data type	Value
Impedance	3.172+j25.615 Ω
Impedance/km	0.0541+j0.4371 Ω/km
Susceptance	187.8 μS
Susceptance/km	3.204 μS/km
Temperature	-51.25°C
Average Height	1.49 m

Table 10.4: The output from the model

The calculated value of the resistance is lower than the reference value. The resulting conductor temperature was there fore calculated to be -51.25℃ which was not considered to be realistic value. Implementing the weather parameters in Table 10.3 and the load current into the following equation earlier presented in Chapter 7

$$T = T_\infty + \frac{I^2(A + BT_\infty) + \epsilon_s D Q_s'}{\pi h D + \epsilon_i \pi D \sigma E - I^2 B} \quad [^\circ\text{C}]$$

results in a estimated conductor temperature of 11.9℃ which is considered to be much reasonable value considering the cooling effects, wind and air temperature. A possible reason for this difference in the conductor temperature will be discussed in the conclusion of this chapter. Implementing the previously calculated temperature of -51.25℃ into the model will not give a realistic value of the individual spans in order of comparing with actual measurements.
In stead the temperature of the conductor which is estimated by the weather parameters and loading is used and the result is shown in the following table.

Span nr.	Clearance	Measured Clearance	Difference
11	14.91 m	10.66 m	4.25 m
16	15.09 m	10.03 m	5.06 m
17	19.29 m	17.89 m	1.40 m

Table 10.5: The output from the model compared with measured values.

There is a significant difference in the measured value and the modelled value of the clearance and the accuracy is

$$accuracy = \frac{10.03}{15.10} \cdot 100\% = 66.42\ \%$$

The average height is calculated according to the susceptance value. The result of 1.49 m average height would mean that the conductor should be laying on ground for a large part of the BR1 connection.

10.4 Conclusion

The calculated value of the conductor temperature of -51.25℃ is not realistic as earlier mentioned. The reason for this could be wrong reference resistance of the conductor. In Appendix C a measurement of the impedance with OMICRON CPC100 and CP CU1 is described. The measurements where conducted by Landsnet's employees in April 2013. The resulting value of the resistance proofs to be considerably lower than the applied reference resistance. The reason for this difference in resistance is that a part of the BR1 connection was reconstructed as a 420 kV line which has a resistance value of 0.04335 Ω/km. This information was set forth by Landsnet in the final stages of the project period. By running the model with the new parameters also resulted in a value which is not considered to be realistic. Possible explanation of this could be error in the measurements. The PMU measures the voltage by ±0.125% accuracy and the current by ±0.5% accuracy.[9] The CP CU1 along with CPC 100 measures the impedance with accuracy of 0.3%.[23] By computing the impedance varying the voltages and currents according to the accuracy, results in a maximum impedance of 0.0594 Ω/km and a minimum impedance of 0.0489 Ω/km. The following equation is a derivation of Equation 9.14 and is used for computing the conductor temperature using resistance measurements.

$$T = \left(\frac{R}{R_0} - 1\right)\left(\frac{1}{\alpha}\right) + T_0 \qquad [^\circ C]$$

Comparing the value of the conductor temperature implementing the maximum value of the impedance and the minimum value of the impedance, results in a temperature difference of 47.2℃ for the conductor.

The impedance was measured with 0.3% accuracy which could result in a decrease in impedance from 0.0681 Ω/km to 0.0679 Ω/km at 2℃. The conclusion is there fore that the measurement of the impedance is not a desirable method when estimating the conductor temperature. The value required from the weather parameters and loading will there fore be used in the model.

Comparing the clearance measurements with the clearance from the model resulted in very large difference as can be seen in Table 10.5. There are number of reasons for this difference, for one the landscape underneath the transmission line is not homogeneous as earlier mentioned. The model only uses the height of one mast for computing the clearance, the mast at the opposite end of the span is possible higher or lower than the mast applied in the model.

Finally the average height of the transmission line is computed according to the susceptance value resulting in height which obviously is not correct. The load of the line at the time of measurements was 229.9 MVA which is 75% of the static line rating of BR1 and the weather conditions suggest a rating around 500 MVA at the measuring point. The loading of the line is there fore less than 50% of the maximum.

11 Sensitivity Analysis

In this chapter a sensitivity analysis will be conducted where the variables of the model will be varied in order to see the deviation of the results of the model.

The input parameters to the model are the magnitudes and angles of the currents and voltages from both ends of a transmission line. It is there fore interesting to explore the deviation of the parameters which were of interest in Chapter 10, the resistance and the susceptance. For this analysis the parameters acquired previously in Chapter 10 are varied. The calculations will be carried out according to previously introduced methods.
The deviation will be done by presuming larger error than previously was accounted for in the conclusion of Chapter 10. This is done to see the tendency of the parameters better. In Figure 11.1 the magnitude of the sending end voltage is varied by ± 0.5 kV.

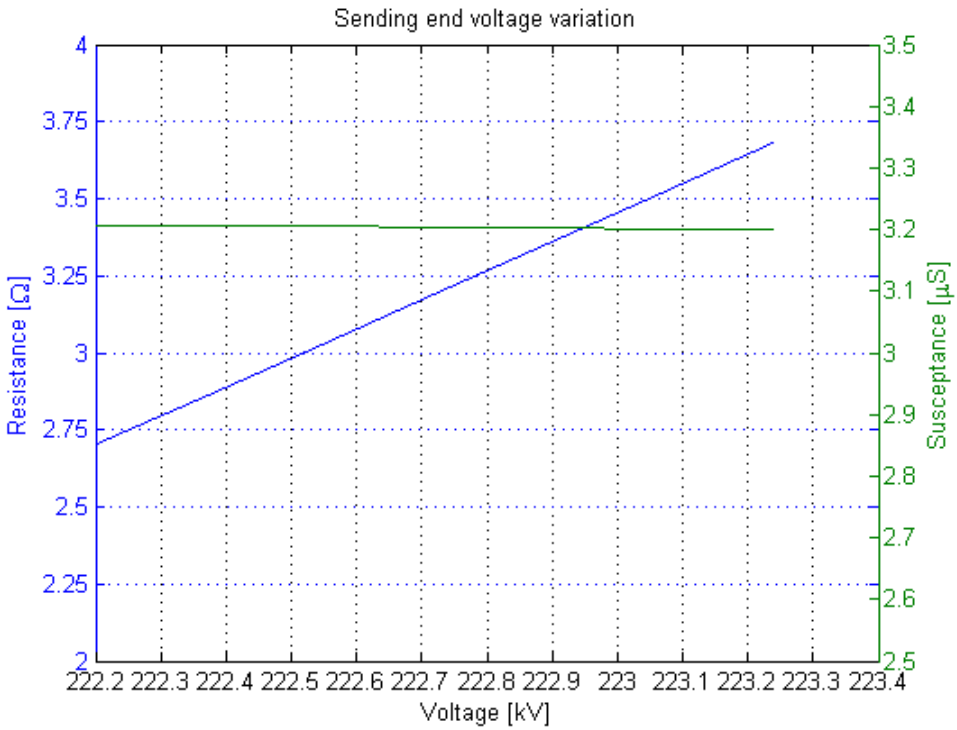

Figure 11.1: Variation of the sending end voltage.

The resulting variation of the resistance and susceptance can be seen in table 11.1. The variation has

big effect on the resistance value opposite to the susceptance where the variation has little effect. The value of the resistance is used to evaluate the conductor temperature there fore it is interesting to see how much impact the variation has on the temperature of the conductor. The variation of the sending end voltage can there fore result in a possible 75.08℃ temperature difference using the same method as in previous chapter. The same is done for the susceptance where the resulting average height for the susceptance values are compared. The variation of the sending end voltage can there fore result in a possible 2 cm average height difference.

	MIN	MAX	Difference
Resistance	2.701 Ω	3.680 Ω	75.08℃
Susceptance	3.200 μS	3.207 μS	2 cm

Table 11.1: Maximum and minimum value of the resistance and susceptance from the variation.

In Figure 11.2 the receiving end voltage is varied by ±0.5 kV as in the case of the sending end voltage. The results are similar where the resistance varies more than the susceptance.

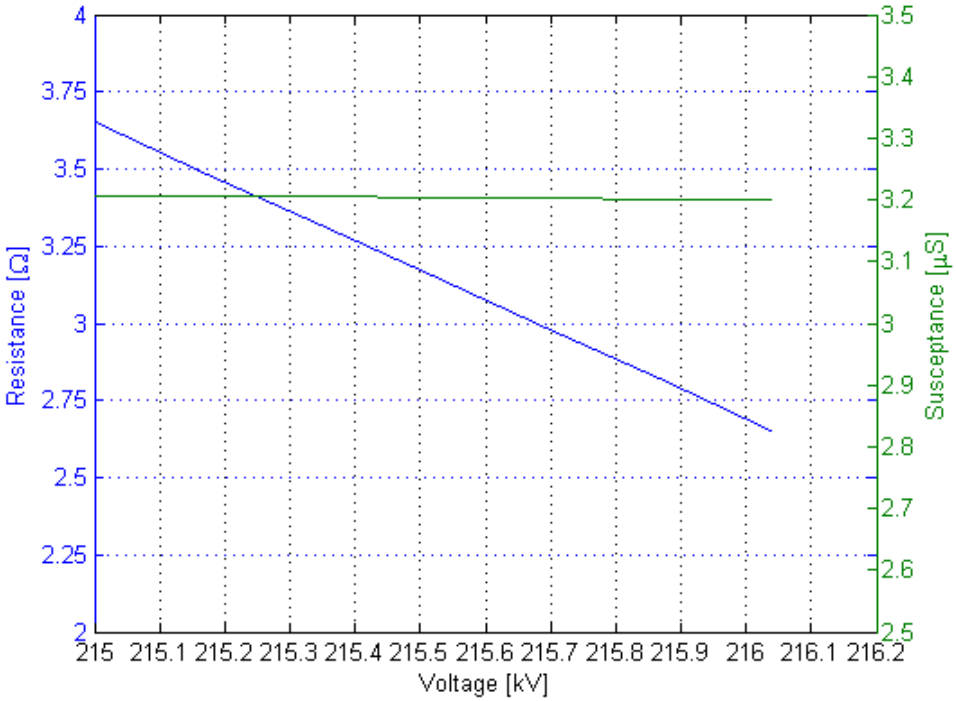

Figure 11.2: Variation of the receiving end voltage.

In Table 11.2 the results of the receiving end voltage variation can be seen. The variation of the voltage could result in a temperature difference of 76.38℃ for the conductor. The variation does however not impact the susceptance value extensively.

	MIN	MAX	Difference
Resistance	2.655 Ω	3.651 Ω	76.38℃
Susceptance	3.201 μS	3.207 μS	2 cm

Table 11.2: Maximum and minimum value of the resistance and susceptance from the variation.

The sending end current magnitude is varied with ±10 A in Figure 11.3.

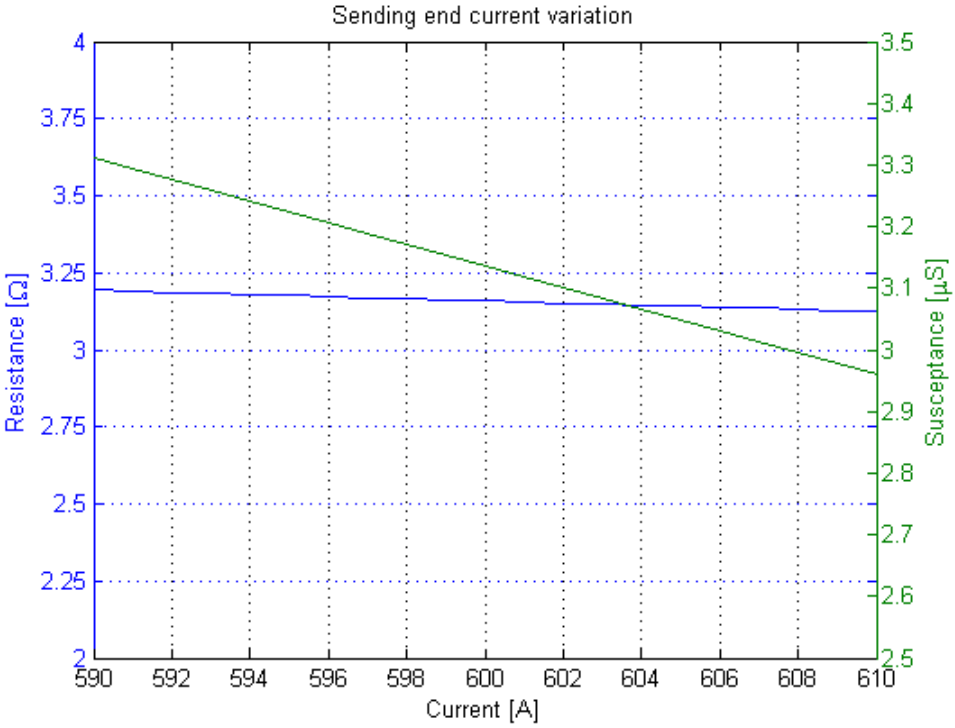

Figure 11.3: Variation of the sending end current magnitude.

The resulting variation in the resistance and susceptance can be seen in Table 11.3. The variation does not have large effect on the conductor temperature compared to the voltage variation. However the variation does have impact on the susceptance value and there fore the average height of the conductor.

	MIN	MAX	Difference
Resistance	3.125 Ω	3.193 Ω	5.21℃
Susceptance	2.961 μS	3.311 μS	123 cm

Table 11.3: Maximum and minimum value of the resistance and susceptance from the variation.

The receiving end current magnitude is varied with ±10 A as done previously for the sending end current magnitude. The result can be seen in Figure 11.4.

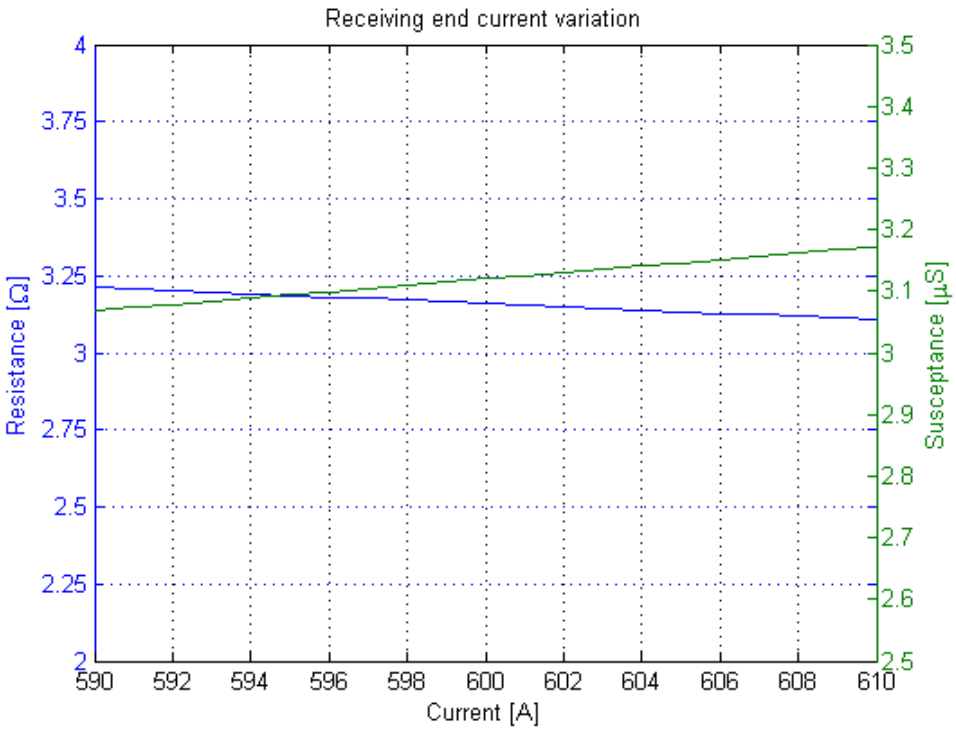

Figure 11.4: Variation of the receiving end current magnitude.

The resulting variation can be seen in Table 11.4. The variation of the receiving end current does not have as large impact on the model results as the variation of the other parameters previously displayed.

	MIN	MAX	Difference
Resistance	3.108 Ω	3.213 Ω	8.05℃
Susceptance	3.068 μS	3.172 μS	36 cm

Table 11.4: Maximum and minimum value of the resistance and susceptance from the variation.

Now the variations of the voltages and currents magnitudes have been analysed the next step is to look at the angles. In Figure 11.5 the sending end voltage angle is varied by $\pm$ 1°.

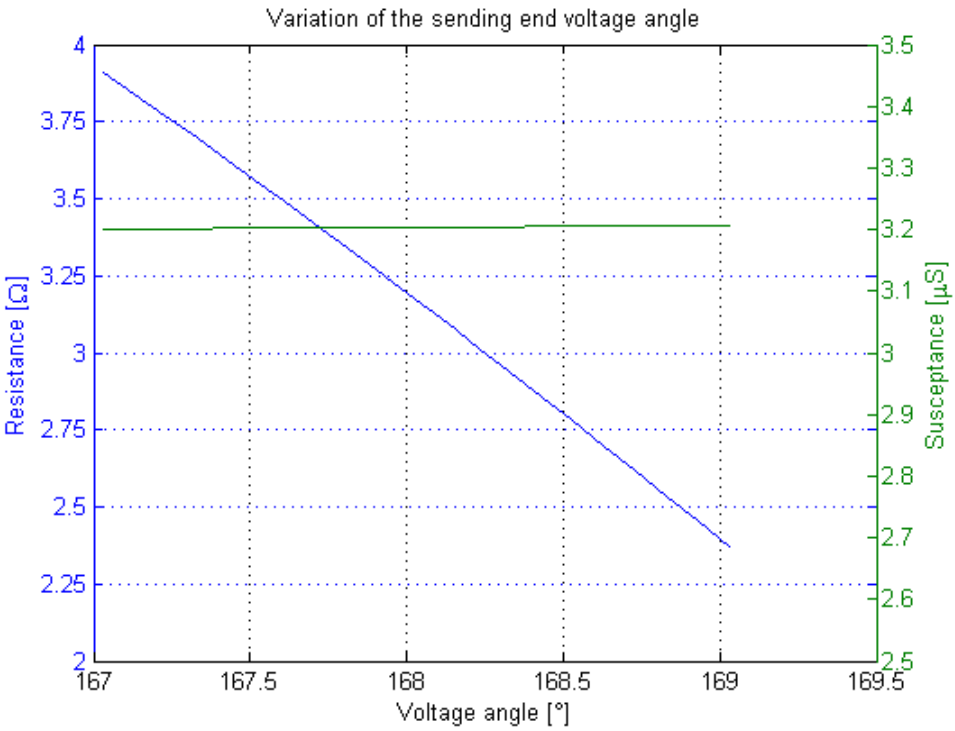

Figure 11.5: Variation of the sending end voltage angle.

In Table 11.5 the result of varying the sending end voltage angle are displayed. The resistance value changes very much resulting in a temperature deviation of 118.25℃. The changes in the susceptance does however not change in order to have any impact on the model results.

	MIN	MAX	Difference
Resistance	2.369 Ω	3.911 Ω	118.25℃
Susceptance	3.201 μS	3.207 μS	2 cm

Table 11.5: Maximum and minimum value of the resistance and susceptance from the variation.

In Figure 11.6 the receiving end voltage angle is varied the same way the sending end voltage angle or by $\pm$ 1°.

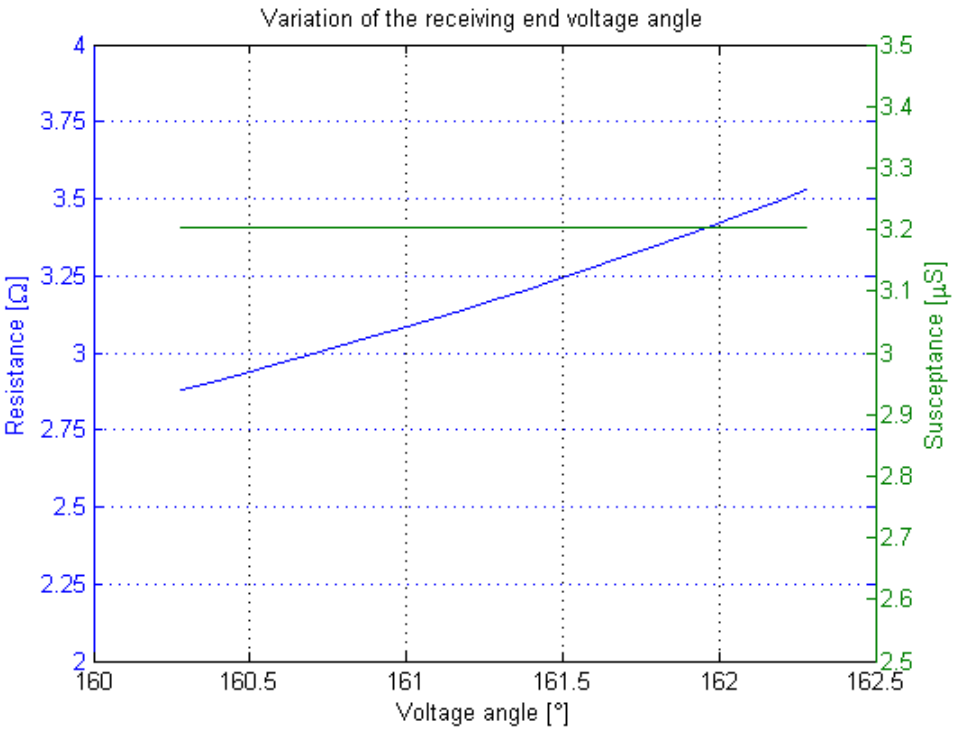

Figure 11.6: Variation of the receiving end voltage angle.

The variation of the receiving end voltage angle also has effect on the resistance but not as severe impact as the change in the sending end voltage angle. The variation of the receiving end voltage has almost no impact on the susceptance value as can be seen in Table 11.6.

	MIN	MAX	Difference
Resistance	2.878 Ω	3.528 Ω	49.77℃
Susceptance	3.203 μS	3.204 μS	0 cm

Table 11.6: Maximum and minimum value of the resistance and susceptance from the variation.

In Figure 11.7 the sending end voltage angle is varied by ±0.5°. The variation is limited to ±0.5° because of the variation of the susceptance value.

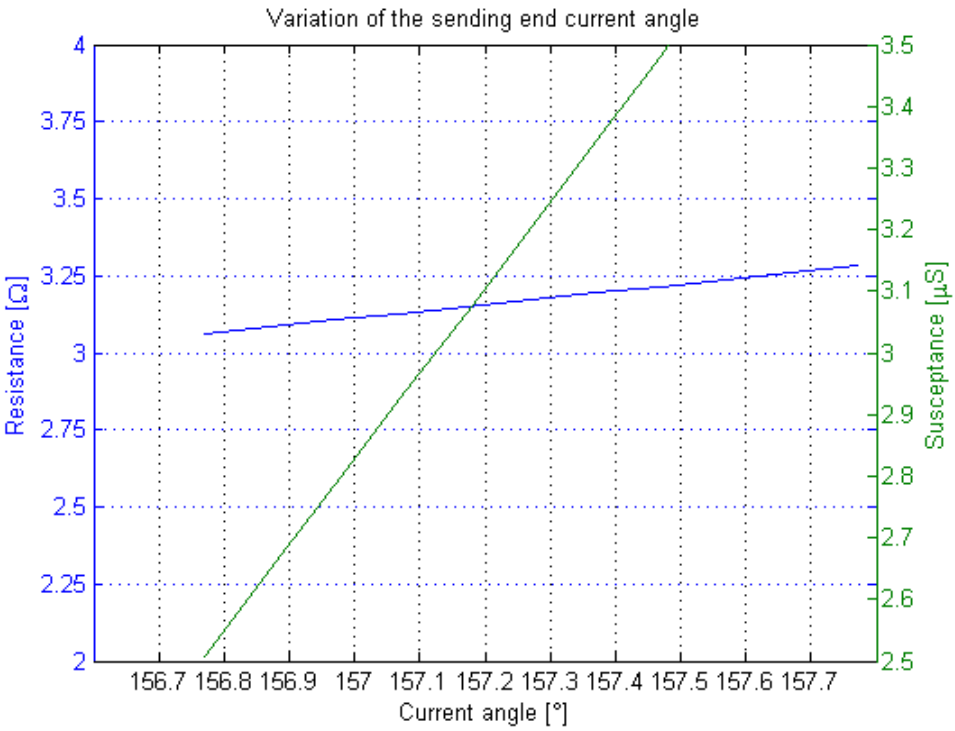

Figure 11.7: Variation of the sending end current angle.

In Table 11.7 the results of varying the sending end current angle is seen. The interesting change lies in the susceptance value as the expected deviation of the average height exceeds 22 m, which is the average height of the mast in the BR1 connection.

	MIN	MAX	Difference
Resistance	3.063 Ω	3.281 Ω	16.72℃
Susceptance	2.507 μS	3.482 μS	+22 m

Table 11.7: Maximum and minimum value of the resistance and susceptance from the variation.

In Figure 11.8 the receiving end current angle is varied by $\pm 0.5°$ as was done for the sending end current angle.

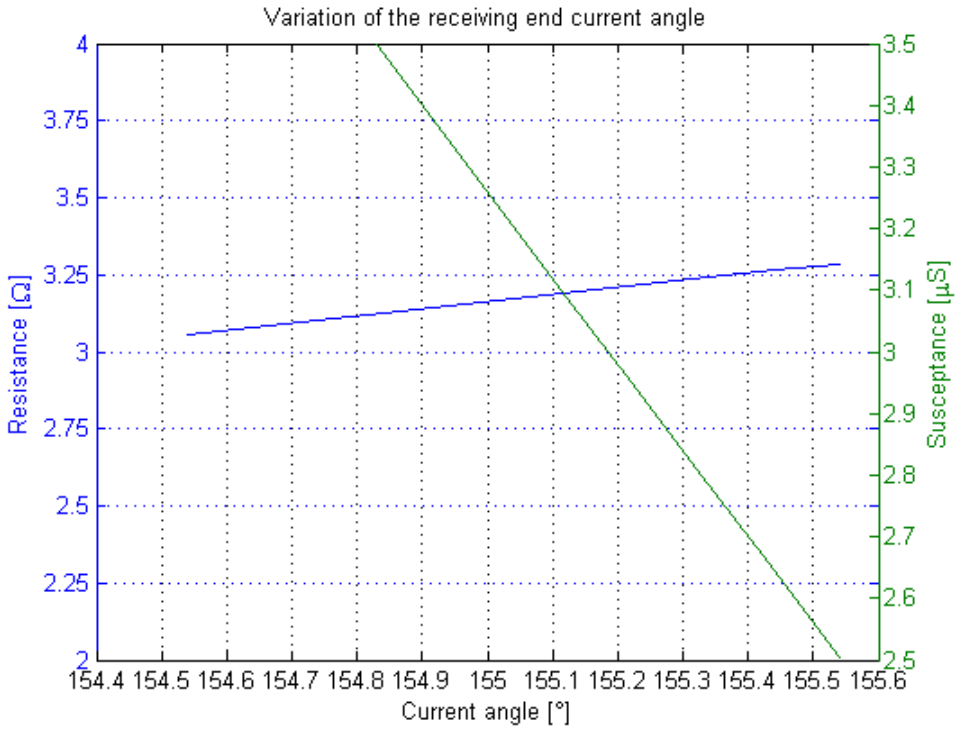

Figure 11.8: Variation of the receiving end current angle.

The variation for the receiving end current angle results in similar deviation as for the sending end current angle.

	MIN	MAX	Difference
Resistance	3.057 Ω	3.286 Ω	17.56℃
Susceptance	2.505 μS	3.483 μS	+22 m

Table 11.8: Maximum and minimum value of the resistance and susceptance from the variation.

Now all the input parameters to the model have been varied. It is clear that changes to the voltage magnitude and angle result in relatively large changes to the resistance measurement thus having severe impact on the conductor temperature estimation. Changes on the current magnitude and angle has effect on the susceptance value which results in change of the average height of the conductor. The angle variation has much more affect on the susceptance value compared to the current magnitude variation. A relatively small change in the current angle results in large deviation of the average height of the conductor.
In order to see the expected value of the susceptance the average height of the conductor is plotted against the susceptance value in Figure 11.9. From the figure the expected value of the susceptance is 2.6 - 2.7 μS. Looking at Figure 11.8 the variation of the current angle should be less than $\pm 0.1°$ in order to be within that region.

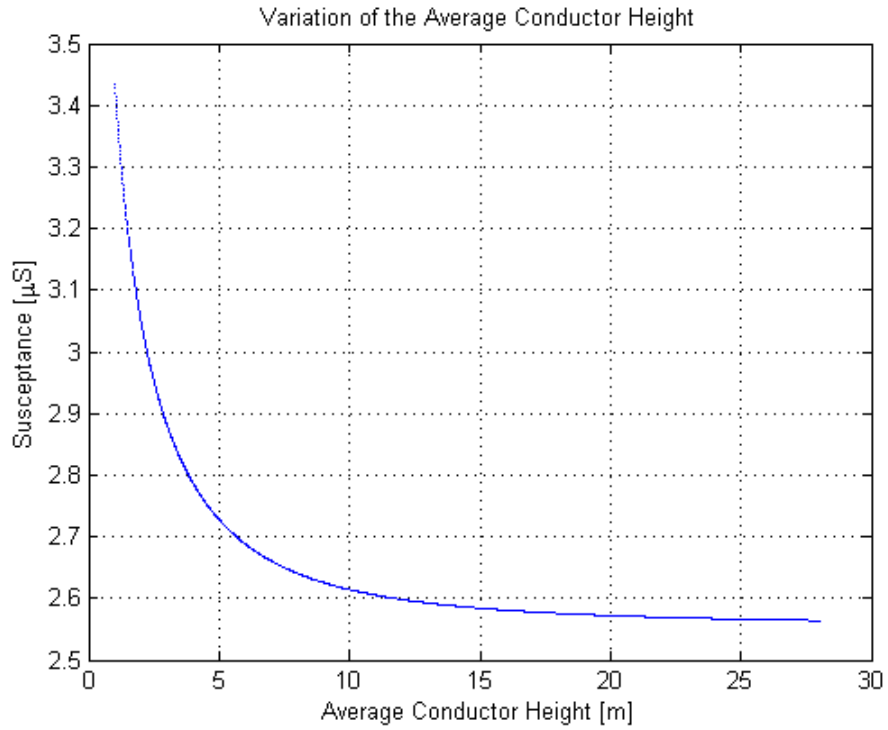

Figure 11.9: Variation of the average height of the conductor.

In Figure 11.10 the resistance of the conductor is varied and compared to the calculated conductor temperature.

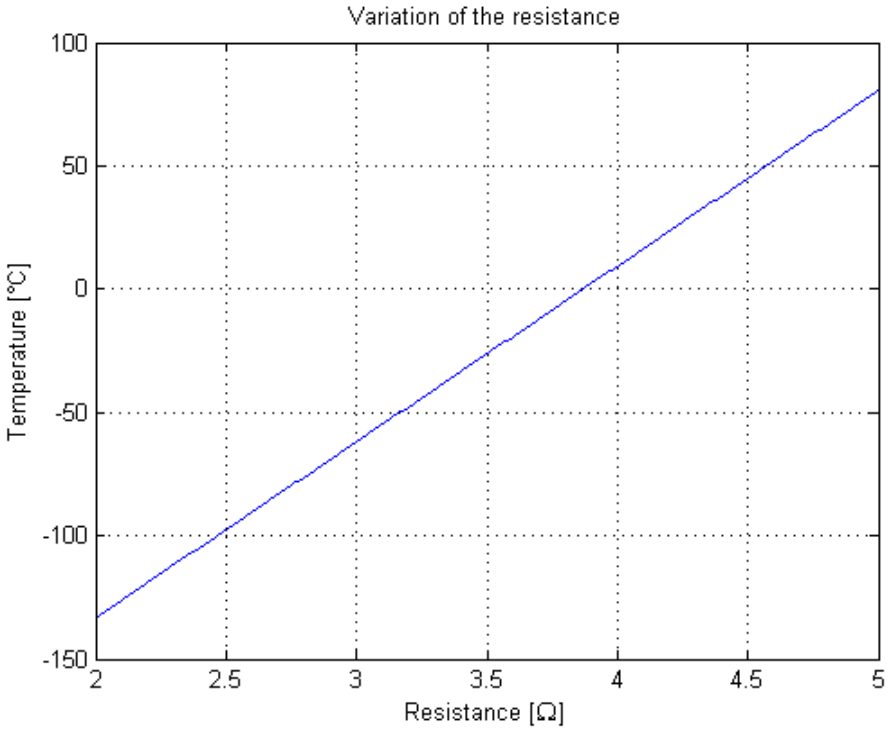

Figure 11.10: Variation of the resistance compared with calculated conductor temperature.

From looking at the figure it is clear that the expected resistance of the BR1 connection is to be around 4 Ω for conductor temperature of 10℃.
In Figure 11.11 the resistance of the conductor is varied and compared to the calculated susceptance of the OHL.

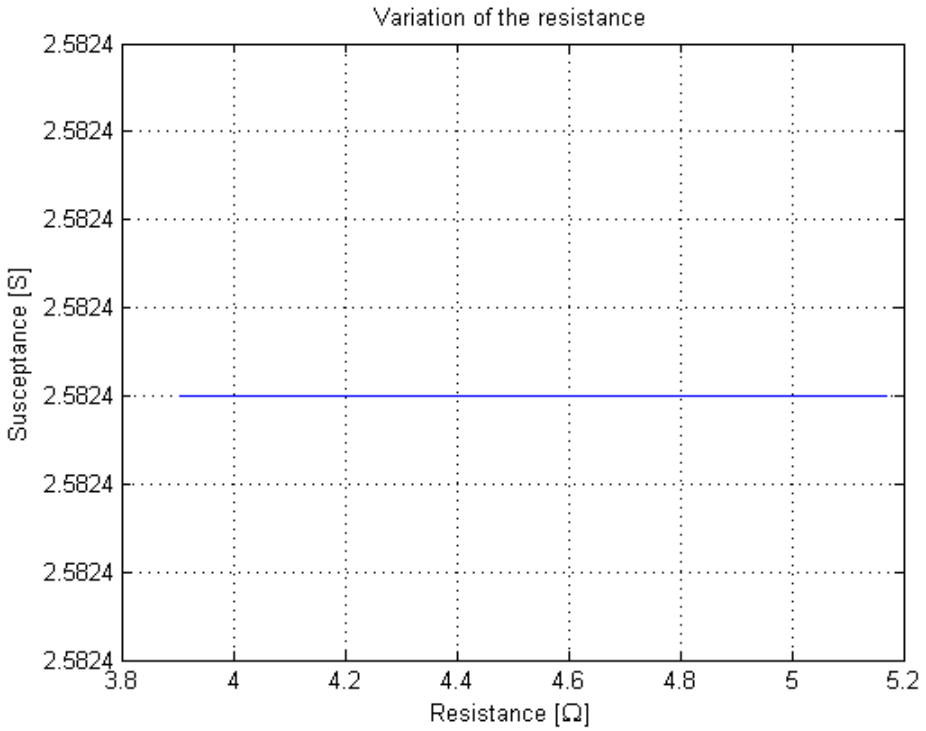

Figure 11.11: Variation of the resistance compared with susceptance.

It is clear that the value of the susceptance is not dependent on the resistance value as the variation of the resistance demonstrates in Figure 11.11. In beginning of Chapter 5 the definition of admittance was presented as the reciprocal of the impedance which would mean that the susceptance value is dependent on the resistance value according to following equation.

$$B = -\frac{X}{R^2 + X^2} \quad [\text{S}]$$

The reason for this is that the computed admittance from the model is only the shunt admittance of the transmission line and the impedance is the series impedance.
The parameters are not expected to deviate as much as the presented data indicates as the accuracy of the measuring device is expected to be higher than the deviation indicates. The tendency of the parameters is however clear and a small deviation of some parameter such as the current angle will result in a misleading outcomes.

12 DigSilent Powerfactory Simulation

In this chapter the model will be tested using the DigSilent Powerfactory by setting up different scenarios.

According to previous Chapter 11 the variation of the resistance had no effect on the value of the susceptance. It is there fore interesting to perform a load flow of a simple overhead line in order of simulating the expected parameters from a PMU unit. In Figure 12.1 the setup in DigSilent Powerfactory is displayed. It is a simple setup as the only purpose of the setup is to test the BR1 connection in order to see the behaviour of the voltages and currents. In stead of using the data for the spans and horizontal tension it is assumed that every span is level and the length is equal as well. The same applies to the horizontal tension.

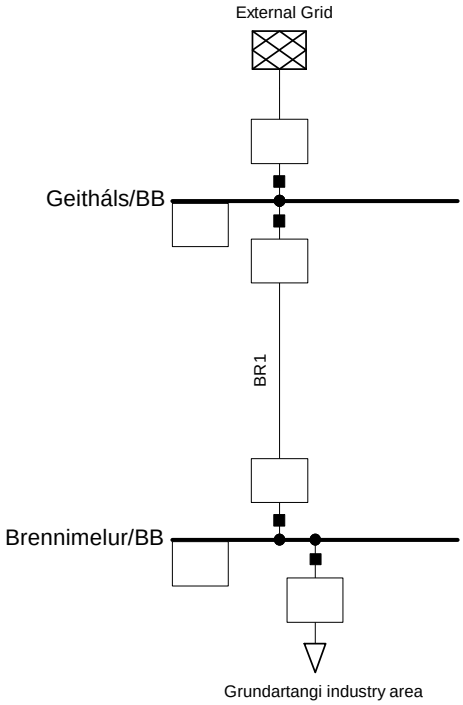

Figure 12.1: The setup of the grid.

The BR1 connection is connected to the busbars which represents the substations, Geitháls and Brennimelur. The busbar at Geitháls is connected to an external grid which supplies the rest of the grid connected. The busbar at Brennimelur is connected to a load which represents the amount of energy

the industry area at Grundartangi is supplied by the BR1 connection.

In Figure 12.2 the data of the mast is implemented to the DigSilent Powerfactory model. The options of how many line circuits, how many earth wires and to indicate if the line is transposed or not. The BR1 connection contains one line circuit, no earth wires are used in the model as they are only close to the substations and there fore they are neglected and the line is not transposed. Information about input mode, earth resistance and the type of conductor have to be applied.

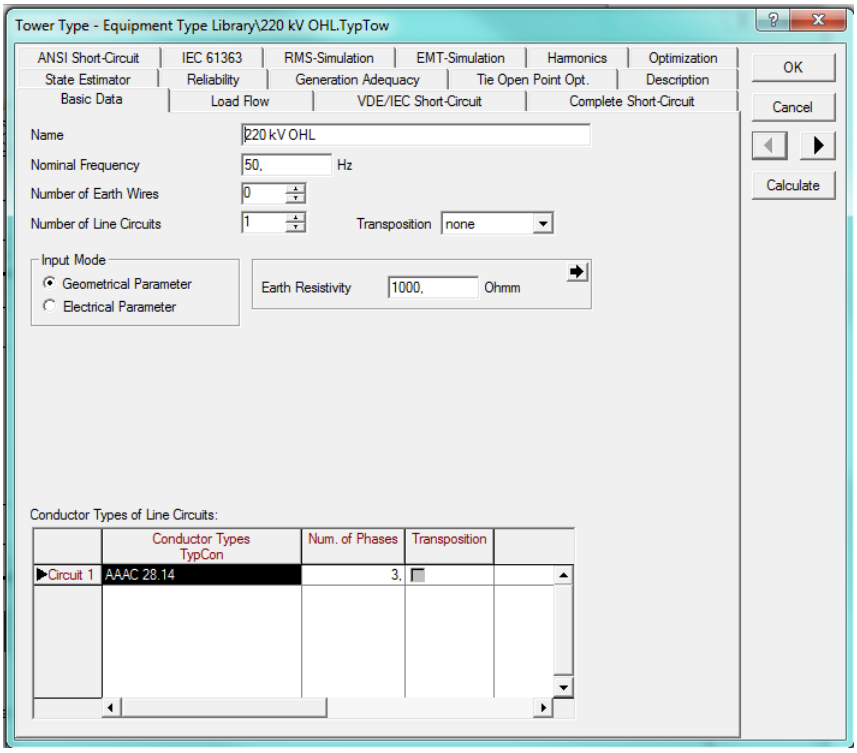

Figure 12.2: Implementation of the data for the BR1 connection.

The implemented data is the same as for the BR1 connection described in Chapter 2. The input mode is selected to be geometrical parameters which is described later. The value of earth resistivity is chosen to be 1000 Ωm according to reference [24]. The type of conductor will be implemented later in this chapter. In Figure 12.3 the dimensions of the overhead lines are implemented to the model. The parameters are implemented as (x,y) coordinates according to Figure 12.4.

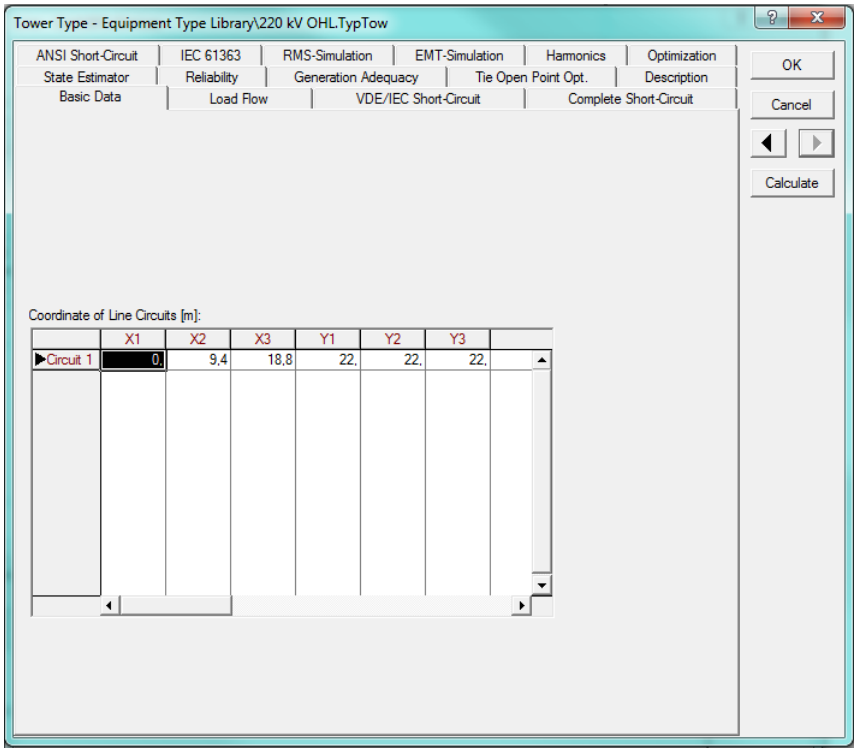

Figure 12.3: Implementation of the conductor coordinates.

In Figure 12.4 the dimensions of the conductor position can be seen.

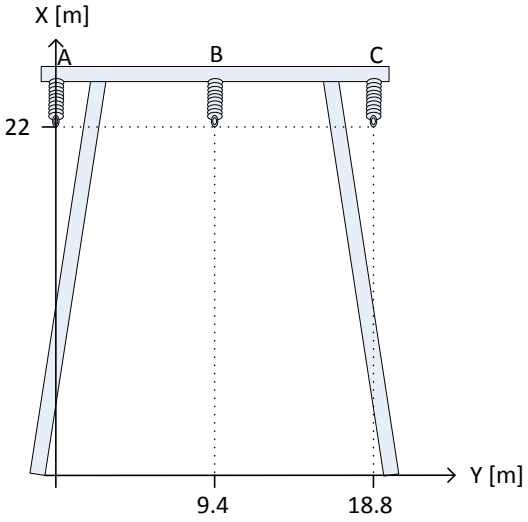

Figure 12.4: Dimensions of the conductor position.

In Figure 12.5 the data for the conductor is implemented into the model according to the data presented in Chapter 2. The nominal voltage, nominal current, DC-resistance and the conductor dimensions are specified

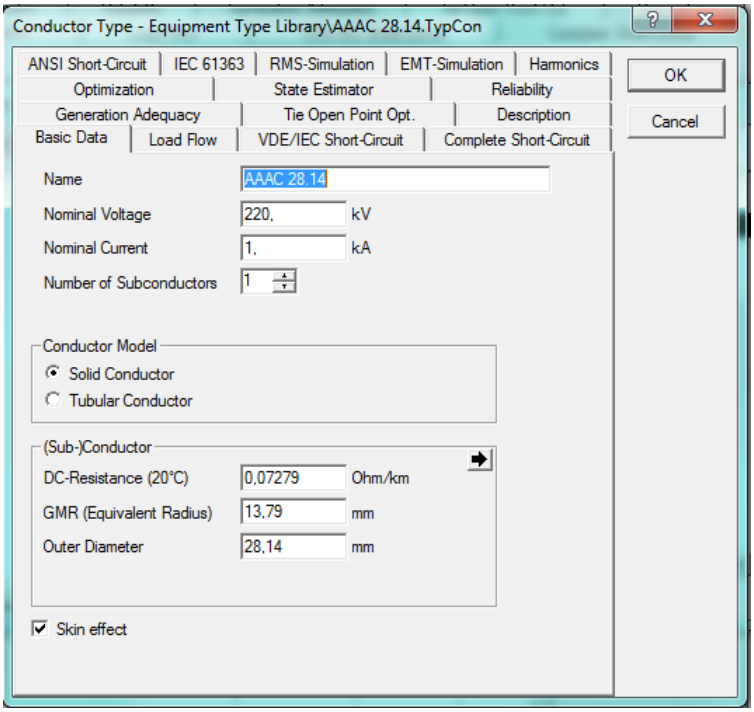

Figure 12.5: The conductor data implementation.

The load connected to the busbar at Brennimelur is now varied in order to see if the value of the calculated susceptance changes. A load flow is performed with 100+j20 MVA load, 200+j20 MVA load and 300+j20 MVA load. The resistance is also kept constant at 0.07279 Ω/km.

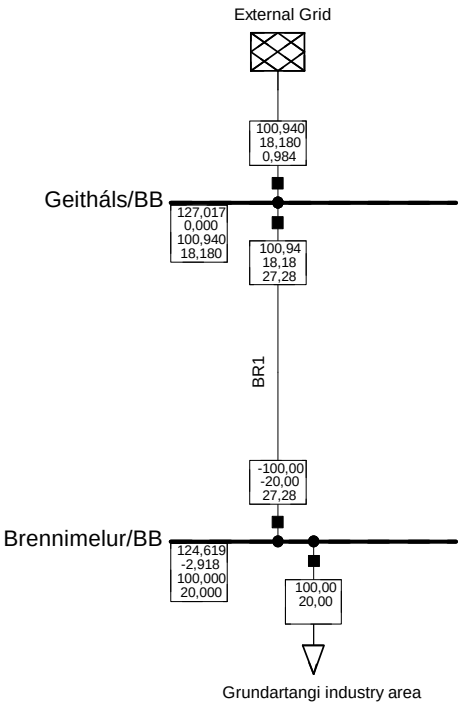

Figure 12.6: 100+j20 MVA load at Grundartangi

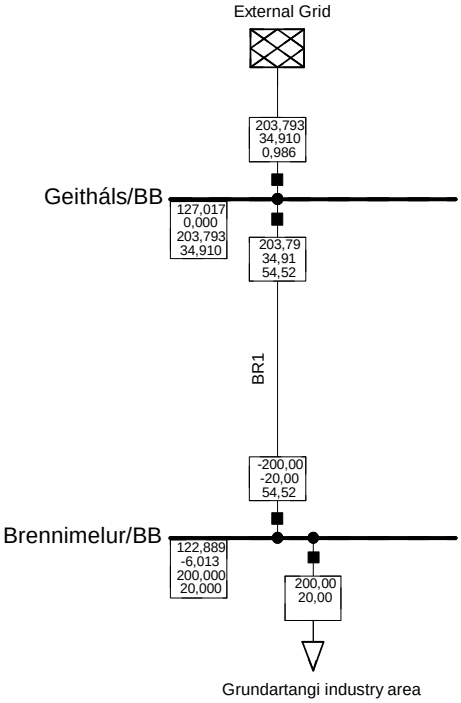

Figure 12.7: 200+j20 MVA load at Grundartangi

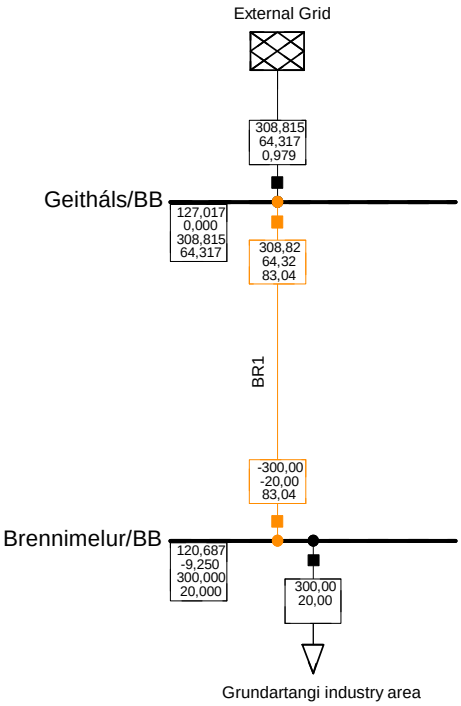

Figure 12.8: 300+j20 MVA load at Grundartangi

From the DigSilent Powerfactory simulation the voltages and currents, both magnitudes and angles can be acquired which are then implemented into the model described in Chapter 9. The resulting value of

the susceptance and the average height is seen in Table 12.1.

Loading [MVA]	Susceptance [μS]	Average conductor height [m]
100+j20	2.6235	9.17
200+j20	2.6240	9.13
300+j20	2.6234	9.17

Table 12.1: Output from the model.

It is clear that the effect of increased loading does not affect the value of the susceptance of any significant degree.
Next the same analysis is conducted with a small change of keeping the resistance constant at 0.06279 Ω/km which reduces the value of the total resistance for the BR1 connection from 4.27 Ω to 3.68 Ω.

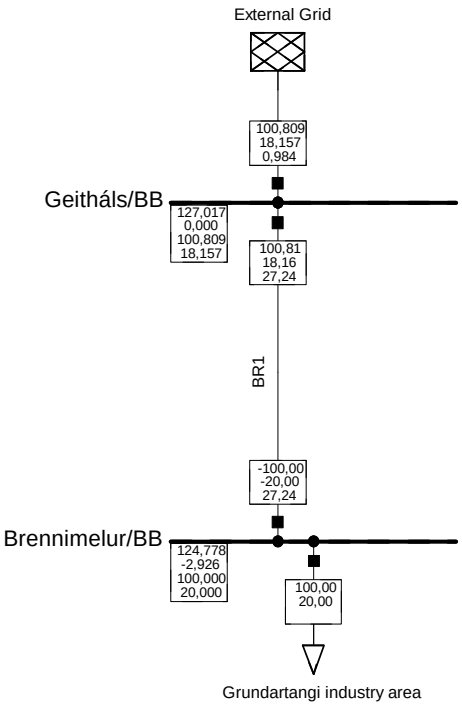

Figure 12.9: 100+j20 MVA load at Grundartangi

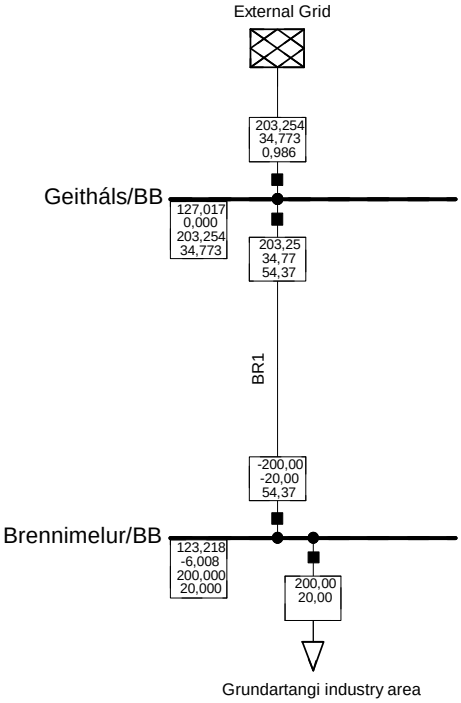

Figure 12.10: 200+j20 MVA load at Grundartangi

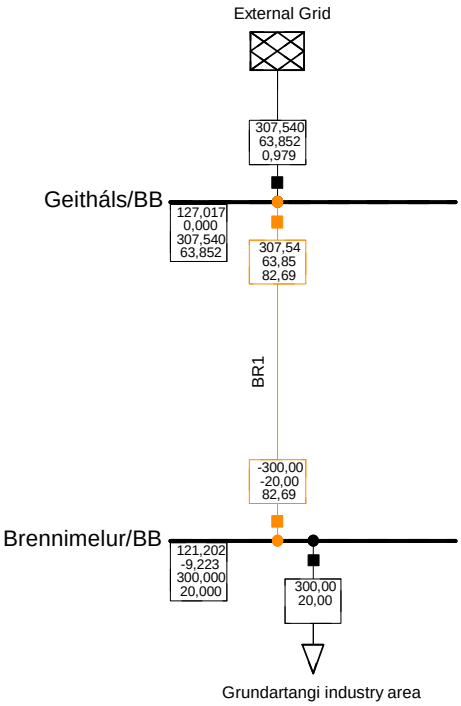

Figure 12.11: 300+j20 MVA load at Grundartangi

The simulated values are implemented into the MATLAB model and the results are displayed in Table 12.2.

Loading [MVA]	Susceptance [μS]	Average conductor height [m]
100+j20	2.6235	9.17
200+j20	2.6229	9.21
300+j20	2.6239	9.14

Table 12.2: Output from the model.

The results show that the variation has very little effect on the susceptance value. The value of the susceptance is similar the results from the previous simulation. Finally the analysis is conducted by increasing the resistance to 0.8279 Ω/km which increases the value of the total resistance of the BR1 connection to 4.85 Ω.

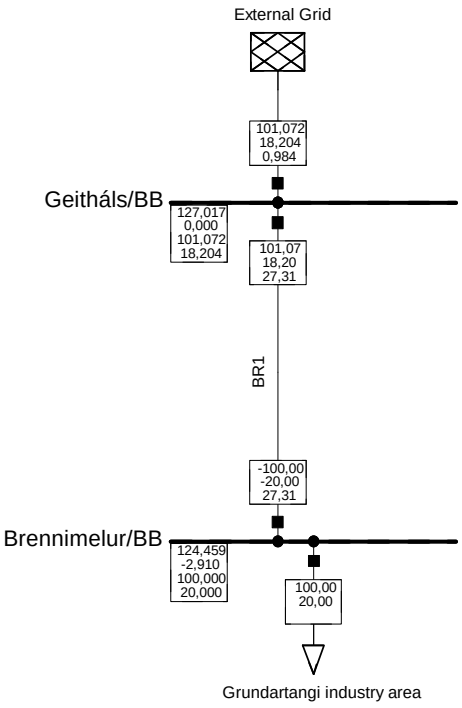

Figure 12.12: 100+j20 MVA load at Grundartangi

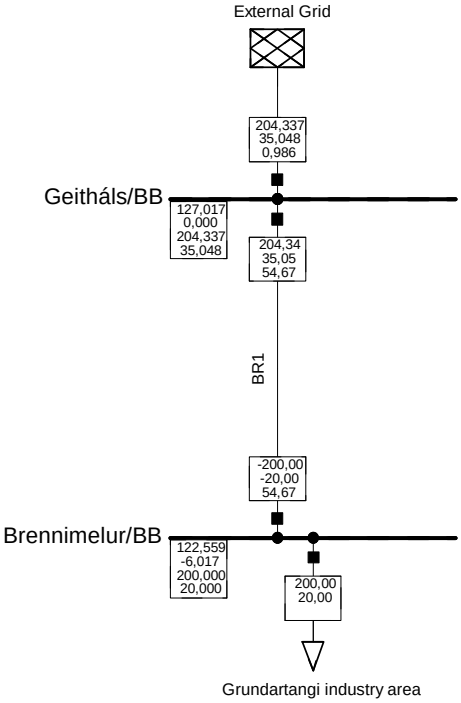

Figure 12.13: 200+j20 MVA load at Grundartangi

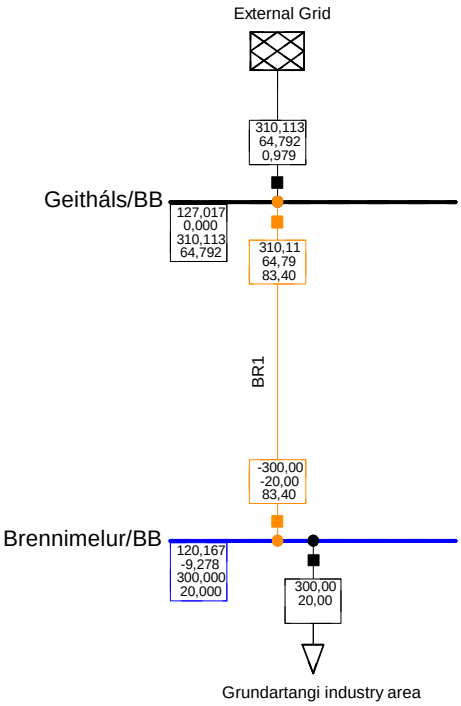

Figure 12.14: 300+j20 MVA load at Grundartangi

The simulated values are implemented into the MATLAB model and the results are displayed in Table 12.3.

Loading [MVA]	Susceptance [μS]	Average conductor height [m]
100+j20	2.6233	9.18
200+j20	2.6238	9.14
300+j20	2.6238	9.14

Table 12.3: Output from the model.

After performing a load flow of the BR1 connection in the DigSilent Powerfactory and varying both the resistance and the load of the BR1 connection, it is clear that the value of the susceptance does not depend on these parameters directly. This simulation does however not include the heating effect which both increasing the resistance and the load would result in and there fore change the dimensions of the conductors position. The dimensions of the conductors is there fore unchanged through out all the simulations resulting in unchanged value of the susceptance.
The conclusion is that the PMU measurements can in theory be used when determining the average height of a transmission line as the dimensions seem to be the deciding factors of the susceptance value according to the simulation.

IV FINALIZATION

13 Conclusion

The objective of this report was to construct a model which would use measurements from a phasor measurement unit(PMU) for determining the dynamic line rating(DLR) of a transmission line. The relevant theory was presented in problem analysis part of this report covering information about DLR, PMU, susceptance, Maxwell's potential and the use of weather parameters for conductor temperature estimation.

One of the limiting factors for line rating is the clearance to the ground from the conductor. The changes in conductor sag is due to changes in conductor temperature which is a result of different loading or changes in the surroundings. The changes in the surroundings are for example changes in the ambient temperature, wind velocity or wind direction. All of which have great effect of cooling the conductor. By increasing the loading the sag increases and when the affect of cooling reduces, the sag also increases, limiting the capacity of the transmission line. The capacity of the transmission line is dependent on the weather parameter. Increase in cooling of the line results in increased capacity of the line.

The model was constructed as a script in the mathematical tool MATLAB. The input to the model is the relevant parameters of the transmission line enlisted in Chapter 2 and the currents and voltages at each end of the line. From the currents and voltages the impedance and admittance is computed by modelling the transmission line as a π-model, as described in Chapter 5. The susceptance, which is the imaginary part of the admittance, is dependent on the dimensions of the conductor. The existence of the susceptance is due to the capacitive effects which is a result of the distance from the conductor to the ground. This feature is utilised in the model as all the dimensions are known parameters except for the average height of the conductor. A numerical solver is constructed which guesses the average height of the conductor and computes the value of the susceptance. The solver finishes by comparing the computed value of the susceptance to the measured value. When the difference in these two values is below certain defined accuracy the solver stops and returns the value of the average height of the conductor.

When determining the line rating the average height can not be used directly unless the transmission line is homogeneous as well as the landscape. In the BR1 connection which is presented in Chapter 2 neither the transmission line nor the landscape is homogeneous. Conducting a DLR on the BR1 connection can there fore not be done as previously described and an alternative method is required.

The catenary equation was presented in Chapter 6 which describes the relation of line sag with horizontal tension, weight per meter and the span length. The span length is a parameter which does not change for individual span. The weight per meter changes, but of a value to small in order of affecting the results as is described in Chapter 9. The horizontal tension does change as the conductor temperature changes. As is described in Chapter 9 the relationship between the conductor temperature and horizontal tension is linearised. The result is a modified catenary equation which is used to model the BR1

connection. In order of applying the modified catenary equation the average conductor temperature is to be known. As the resistance increases with increased temperature the idea is to utilise the information from the PMU regarding the resistance to compute the average temperature of the conductor. The sag for each span can there fore be computed and the average value acquired from the numerical solver can be compared to the resulting average from the modified catenary equation.
The model is tested using a fixed case and all results indicate the equations have been implemented correctly and the average height is computed with high accuracy.
As the model proofs to work accordingly the next step is to run the model using actual measurements from the BR1 connection. The clearance was measured for three different spans and the data acquired from the PMU was implemented into the model. The first problem with the model was that the conductor temperature estimation could not be used. The measured resistance proofed to be much lower than the resistance at reference point of 20℃. A part of the BR1 connection had been reconstructed as a 420 kV line resulting in different value of the resistance for the entire BR1 connection. The data for that part of the line was first acquired in the last phase of the project period. The impedance had been measured by Landsnet's employees in april 2013 and by implementing the measured data a different temperature was computed from the model but the value was still unrealistic. A decision was there fore made to use the computed temperature from the loading and weather parameters. The computed conductor temperature was 11.9℃ which is considered to be realistic. Running the model using the value of the temperature gained from the loading and weather parameters resulted in a clearance of the conductor for the selected spans which was unfortunately quite different than the measured values and the accuracy was only about 66%. There is a possibility that the measurements acquired for the horizontal tension of the BR1 connection contain some errors. If a measurement, for all the necessary variables of the catenary equation would be conducted for the entire BR1 connection, more accurate result could be acquired. Also by conducting measurements of the clearance for different scenarios could result in a similar variation of the clearance. Thus the difference in the calculated clearance for different scenarios could be the same for the model and for the measured clearance. In that case the model could be used by setting the value of the modelled clearance for the maximum loading of the line as a reference point. In order to change the load of the BR1 connection, another connection needs to be taken out of service. Unfortunately the opportunity for performing such measurement did not occur. The one scenario presented in the case study will there fore be the only scenario tested in this project leaving the verification to the future work on this project. The second problem with the model was that the computed average height of the conductor was only 1.49 m which would indicate that the conductor is laying on the ground for a large part of each span. According to Chapter 11 a little variation in the current angle will result in a relatively large deviation of the susceptance value, thus resulting in large deviation in the average height of the conductor.
The model was tested by implementing the data of the BR1 connection to the simulation program, DigSilent Powerfactory and simulating different scenarios, it came clear that any load and resistance deviation did not affect the value of the susceptance. According to the applied theory the model should work, implementing the data for the BR1 connection to the model does however not result in a realistic values of the average height nor a realistic clearance for the individual spans, which where measured in the case study in Chapter 10. In the problem statement the assumption was made that the existence of the earth wire was neglected as their existence is only close to the substations. As mentioned earlier the value of the susceptance is sensitive to any change in the current, especially the current angle. This assumption

could be the parameter which is affecting the result of the model. Another assumption which was made in the beginning of the project period was to model the circuit as a nominal π-model, the equivalent π-model is more accurate. As the sensitivity analysis indicated the sensitivity of the measurements, using the equivalent π-model could result in different values of the susceptance. The conclusion is there fore that a dynamic line rating model based on the measurements of a phasor measurement unit is not affective in praxis due to sensitivity in the current measurements.

Future Works

For future works on this project could be to implement the model on another connection. A connection which is placed in area of which has more homogeneous landscape in order to prevent any affect the surrounding landscape could have on the results.
As the result of the sensitivity analysis indicates the variation of the current angle has large effect on the susceptance value, the use of equivalent π-circuit model could result in a more accurate results. It would there fore be interesting to compute the impedance and admittance according to the equivalent π-model and compare the resulting suscptance to the value acquired from the nominal π-circuit.
Setting up different scenario and measuring the clearance in order to test the method described in the conclusion. By comparing the difference in of the modelled value of the clearance to the difference in measured value of the clearance for the different scenarios.
Examining the effect of the assumption made in the problem statement of neglecting the existence of the earth wire. This could be done by comparing the value of the susceptance where a earth wire was implemented, to the current model.

A APPENDIX

A Data

The following Table A.1 contains information about each mast in the BR1 connection; height, span length and ...(waiting for info)

Table A.1: The data for the masts in the BR1 connection.[6]

Nr.	Direction	Tension mast	Elevation	Span length	Height		
1.	0.00	1	12.6	288	20.0	20.0	20.0
2	0.00	0	-13.6	388	23.0		24.0
3	0.00	0	0.1	443	26.0		26.0
4	-9.48	1	-7.3	228	17.0	17.0	17.0
5	0.00	0	-8.2	397	20.0		20.0
6	0.00	0	5.0	301	20.0		20.0
7	0.00	0	-17.0	309	18.5		17.0
8	0.00	0	-6.7	393	17.0		16.0
9	0.00	0	-2.3	408	17.0		17.0
10	0.00	0	7.6	337	21.5		20.0
11	0.00	0	-1.9	336	23.0		23.0
12	0.00	0	14.8	359	20.0		21.5
13	25.63	1	23.6	435	20.0	20.0	20.0
14	0.00	0	18.3	397	26.0		27.5
15	0.00	0	12.4	457	26.0		26.0
16	0.00	0	28.0	340	23.0		24.5
17	0.00	0	37.9	276	24.5		27.5
18	0.00	0	-2.3	188	16.0		19.0
19	0.00	0	3.7	430	19.0		21.0
20	0.00	0	10.5	269	26.0		26.0
21	0.00	0	-15.5	185	17.0		17.0
22	0.00	0	-36.8	330	20.0		21.0
23	-21.66	1	2.7	422	20.0	20.0	20.0
24	0.00	0	9.2	342	26.0		27.0
25	0.00	0	11.4	393	23.0		24.5
26	0.00	0	18.9	409	23.0		23.0
27	0.00	0	10.5	306	23.0		23.0
28	0.00	0	3.2	396	23.0		23.0

Continued on next page

Table A.1 – continued from previous page

Nr.	Direction	Tension mast	Elevation	Span length	Height		
29	0.00	0	22.4	415	20.0		20.0
30	0.00	0	13.3	312	27.0		25.0
31	0.00	0	9.3	374	24.0		22.0
32	0.00	0	-2.1	436	20.0		21.0
33	0.00	0	-2.7	434	26.0		26.0
34	0.00	0	14.1	427	23.0		22.0
35	0.00	0	29.5	414	23.0		23.0
36	0.00	0	14.8	206	17.0		17.0
37	0.00	0	-10.1	393	20.0		20.0
38	-42.62	1	-8.4	318	20.0	20.0	20.0
39	0.00	0	-14.7	448	23.0		23.0
40	0.00	0	-6.3	385	23.0		23.0
41	0.00	0	-6.6	413	23.0		23.0
42	0.00	0	-2.8	384	24.0		23.0
43	0.00	0	-11.8	441	26.0		26.0
44	0.00	0	-3.2	414	23.0		23.0
45	0.00	0	-8.6	399	26.0		25.0
46	0.00	0	-4.2	451	23.0		23.0
47	0.00	0	-0.1	399	26.0		26.0
48	0.00	0	-20.5	415	26.0		26.0
49	0.00	0	-12.8	433	26.0		24.0
50	0.00	0	0.4	404	27.0		26.0
51	0.00	0	-11.7	431	23.0		23.0
52	0.00	0	-0.3	394	17.0		17.0
53	0.00	0	16.5	440	26.0		26.0
54	0.00	0	22.6	413	24.0		22.0
55	0.00	0	9.1	428	23.0		24.0
56	0.00	0	24.8	390	25.0		28.0
57	0.00	0	8.0	366	23.0		24.0
58	0.00	0	23.0	352	23.0		23.0
59	0.00	0	19.5	341	17.0		17.0
60	0.00	0	25.5	348	17.0		17.0
61	0.00	0	6.0	374	23.0		23.0
62	-17.85	1	-1.5	378	20.0	20.0	20.0
63	0.00	0	-24.3	451	26.0		27.0
64	0.00	0	-43.5	318	22.0		24.0
65	0.00	0	-43.9	298	24.0		27.0
66	0.00	0	-21.9	411	23.0		23.0
67	0.00	0	-46.8	327	22.0		18.0
68	0.00	0	-28.4	449	25.0		28.0

Continued on next page

Table A.1 – continued from previous page

Nr.	Direction	Tension mast	Elevation	Span length	Height		
69	0.00	0	0.6	417	20.0		20.0
70	0.00	0	-5.1	417	23.0		23.0
71	0.00	0	-14.6	308	26.0		26.0
72	-45.75	1	-13.3	387	20.0	20.0	20.0
73	0.00	0	-18.0	389	26.0		26.0
74	0.00	0	-1.2	446	23.0		23.0
75	0.00	0	-6.7	427	23.0		24.0
76	0.00	0	-7.7	432	23.0		24.0
77	0.00	0	13.4	293	23.0		23.0
78	0.00	0	-11.9	398	23.0		23.0
79	0.00	0	-17.9	445	26.0		28.0
80	0.00	0	0.0	373	26.0		26.0
81	0.00	0	21.5	444	23.0		23.0
82	0.00	0	26.2	224	23.0		23.0
83	39.34	1	66.2	295	14.0	14.0	14.0
84	0.00	0	40.2	226	21.0		20.0
85	0.00	0	5.9	242	17.0		17.0
86	0.00	0	11.8	454	17.0		17.0
87	0.00	0	7.0	270	20.0		21.0
88	0.00	0	-14.3	399	23.0		24.0
89	0.00	0	-19.1	411	20.0		22.0
90	0.00	0	-7.0	366	25.0		27.0
91	0.00	0	-14.5	401	20.0		21.0
92	0.00	0	-4.2	353	17.0		18.0
93	0.00	0	-12.3	253	20.0		20.0
94	-0.03	1	-77.7	425	14.0	14.0	14.0
95	0.08	1	16.3	199	20.0	20.0	20.0
96	0.00	0	32.2	211	18.0		16.0
97	0.00	0	17.2	193	17.0		17.0
98	55.07	1	0.7	209	14.0	14.0	14.0
99	0.00	0	1.8	140	23.0		23.0
100	0.00	0	4.4	136	20.6		17.6
101	0.00	0	-8.0	184	22.0		18.0
102	0.00	0	-2.0	162	22.6		18.6
103	0.00	0	-4.3	136	17.6		15.6
104	0.00	0	-5.3	141	18.6		16.6
105	0.00	0	-12.9	146	19.0		16.0
106	0.00	0	-10.7	134	20.6		17.6
107	3.85	1	-106.9	399	20.0	20.0	20.0
108	-0.10	1	-37.2	391	20.0	20.0	20.0

Continued on next page

Table A.1 – continued from previous page

Nr.	Direction	Tension mast	Elevation	Span length	Height		
109	-40.96	1	19.3	481	17.0	17.0	17.0
110	-49.49	1	-14.5	271	20.0	20.0	20.0
111	0.00	0	10.3	294	17.0		16.0
112	0.00	0	12.1	190	17.0		16.0
113	-16.32	1	24.2	202	20.0	20.0	20.0
114	0.00	0	-13.8	910	58.0	58.0	58.0
115	0.00	0	-7.1	158	58.0	58.0	58.0
116	75.37	1	8.5	319	20.0	20.0	20.0
117	0.00	0	-17.9	278	23.0		24.0
118	0.00	0	-11.0	371	26.0		26.0
119	0.00	0	16.4	329	28.6		25.6
120	-50.55	1	3.4	316	14.0	14.0	14.0
121	0.00	0	-2.1	316	17.0		18.0
122	0.00	0	14.8	232	24.0		22.0
123	0.00	0	2.5	217	20.0		20.0
124	-51.27	1	-12.8	251	20.0	20.0	20.0
125	0.00	0	-30.7	380	24.0		23.0
126	0.00	0	5.2	339	26.0		26.0
127	0.00	0	12.7	374	18.0		17.0
128	0.00	0	13.1	255	19.0		16.0
129	-41.80	1	-3.4	406	20.0	20.0	20.0
130	0.00	0	8.0	181	23.0		23.0
131	28.39	1	11.1	273	17.0	17.0	17.0
132	0.00	0	9.6	283	20.0		21.0
133	-2.88	0	4.8	293	24.0		22.0
134	-2.04	0	-13.3	382	24.0		23.0
135	0.00	0	-9.5	290	21.0		20.0
136	0.00	0	3.3	363	21.0		20.0
137	0.00	0	-1.2	377	24.0		23.0
138	0.00	0	10.0	389	25.0		22.0
139	0.00	0	28.6	350	24.0		23.0
140	0.00	0	-0.7	305	25.0		21.0
141	0.00	0	-6.6	280	21.0		19.0
142	0.00	0	0.4	343	18.0		17.0
143	18.48	1	23.9	381	17.0	17.0	17.0
144	0.00	0	4.0	325	25.0		22.0
145	0.00	0	-5.1	365	23.0		22.0
146	0.00	0	-10.1	349	25.0		21.0
147	36.44	1	88.5	461	22.0	20.0	17.0
148	0.00	0	9.1	332	28.6		23.6

Continued on next page

Table A.1 – continued from previous page

Nr.	Direction	Tension mast	Elevation	Span length	Height	
149	-5.70	0	-10.6	282	23.6	20.6
150	0.00	0	-13.5	595	24.6	23.6
151	-65.82	1	0.0	0	21.0	21.0	21.0

B Linearisation of the horizontal tension

In this chapter the data used for the linearisation for the horizontal tension will be presented and the horizontal tension plotted versus the conductor temperature.

In the following tables the data sets which where acquired by noting down the placement of intersection of the curves for horizontal tension versus the elongation of the conductor as described in Chapter 9. Table B.1 and Figure B.1 represent the section of spans between masts nr.1 to nr.4.

Temperature °C	Tension [MPa]
20	41.50
30	41.29
40	39.73
50	38.15
60	36.40
70	34.68
80	33.40
90	32.07

Table B.1: The data set for section 1

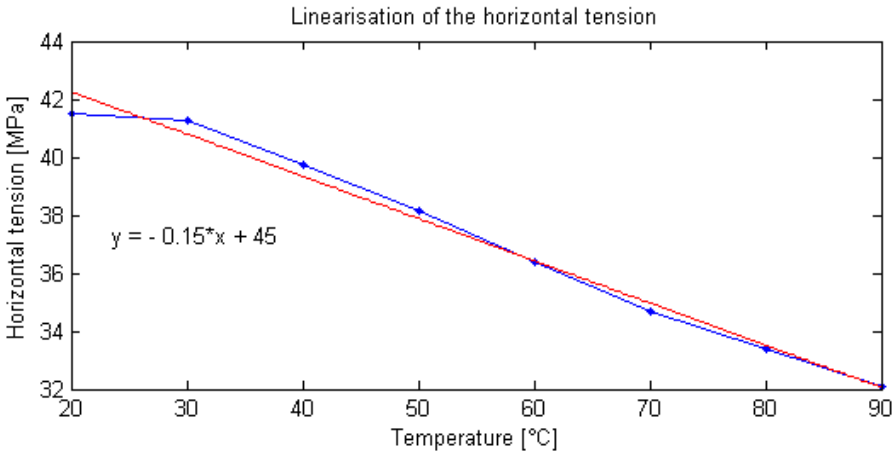

Figure B.1: The plot of data set for section 1

Table B.2 and Figure B.2 represent the section of spans between masts nr.4 to nr.13.

Temperature °C	Tension [MPa]
20	46.00
30	44.70
40	43.15
50	41.37
60	39.60
70	38.20
80	36.73
90	35.25

Table B.2: The data set for section 2

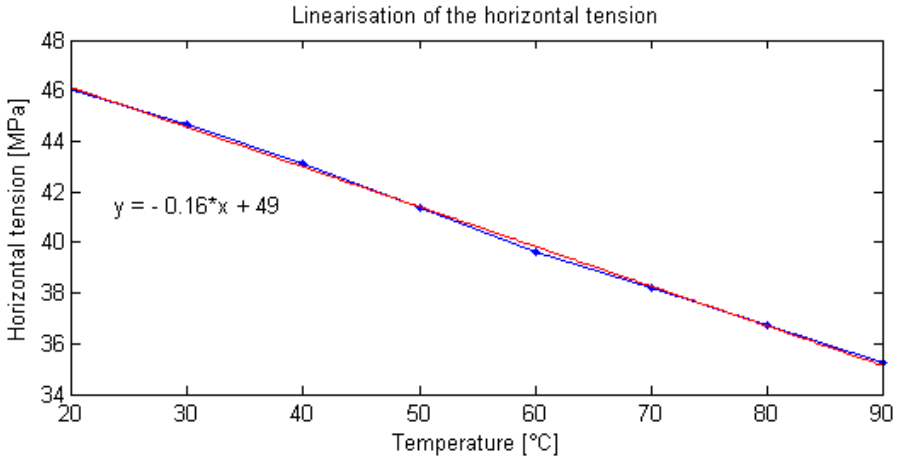

Figure B.2: The plot of data set for section 2

Table B.3 and Figure B.3 represent the section of spans between masts nr.13 to nr.23.

Temperature °C	Tension [MPa]
20	48.75
30	47.09
40	45.36
50	43.97
60	42.65
70	41.30
80	39.95
90	39.00

Table B.3: The data set for section 3

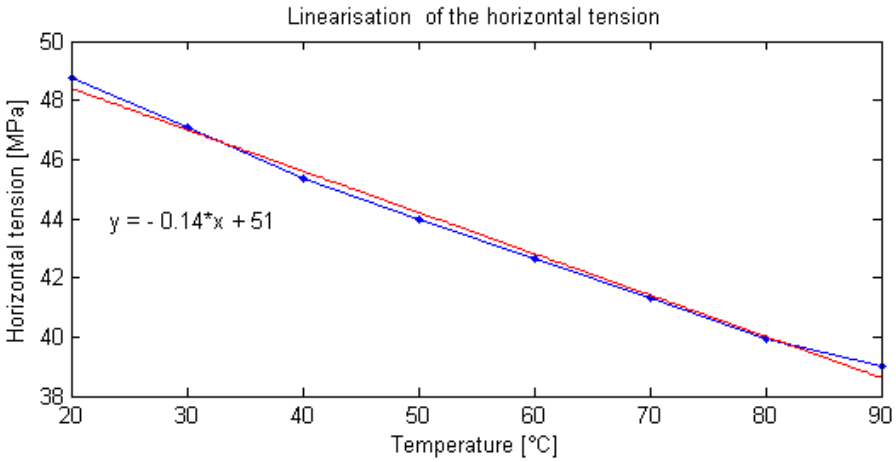

Figure B.3: The plot of data set for section 3

Table B.4 and Figure B.4 represent the section of spans between masts nr.23 to nr.38.

Temperature °C	Tension [MPa]
20	51.00
30	49.27
40	47.66
50	45.97
60	44.44
70	43.14
80	41.82
90	40.48

Table B.4: The data set for section 4

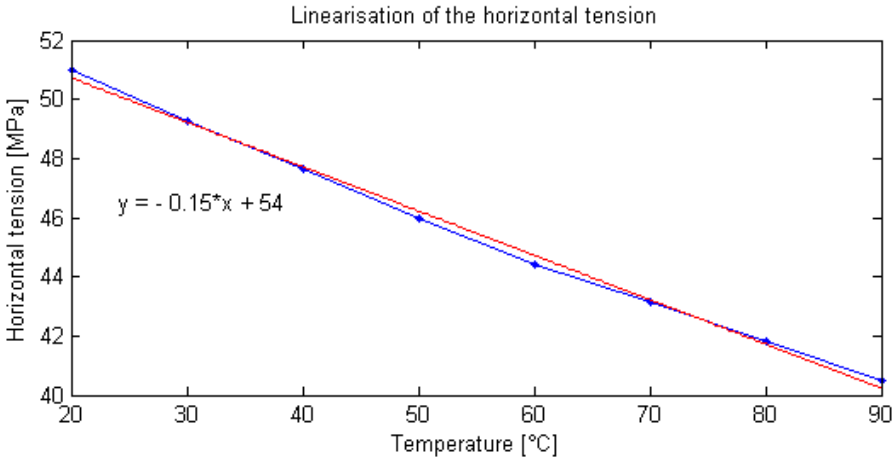

Figure B.4: The plot of data set for section 4

Table B.5 and Figure B.5 represent the section of spans between masts nr.38 to nr.62.

Temperature °C	Tension [MPa]
20	50.88
30	49.18
40	47.62
50	46.00
60	44.54
70	43.32
80	42.08
90	40.83

Table B.5: The data set for section 5

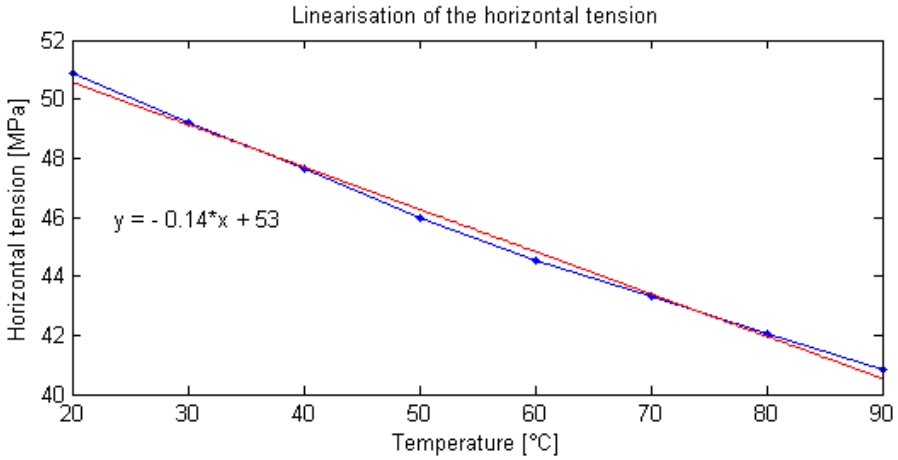

Figure B.5:

Table B.6 and Figure B.6 represent the section of spans between masts nr.62 to nr.72.

Temperature °C	Tension [MPa]
20	48.64
30	46.94
40	45.14
50	43.75
60	42.35
70	40.94
80	39.65
90	38.64

Table B.6: The data set for section 6

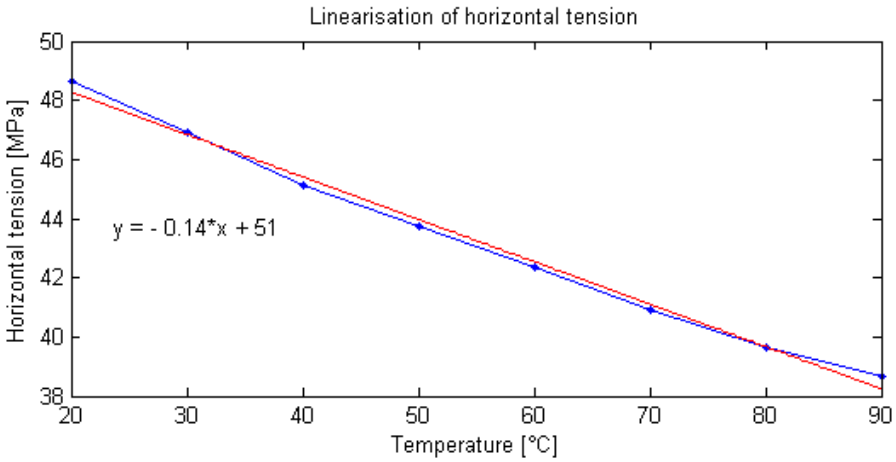

Figure B.6: The plot of data set for section6

Table B.7 and Figure B.7 represent the section of spans between masts nr.72 to nr.83.

Temperature °C	Tension [MPa]
20	49.12
30	47.47
40	45.75
50	44.24
60	42.91
70	41.55
80	40.18
90	39.15

Table B.7: The data set for section 7

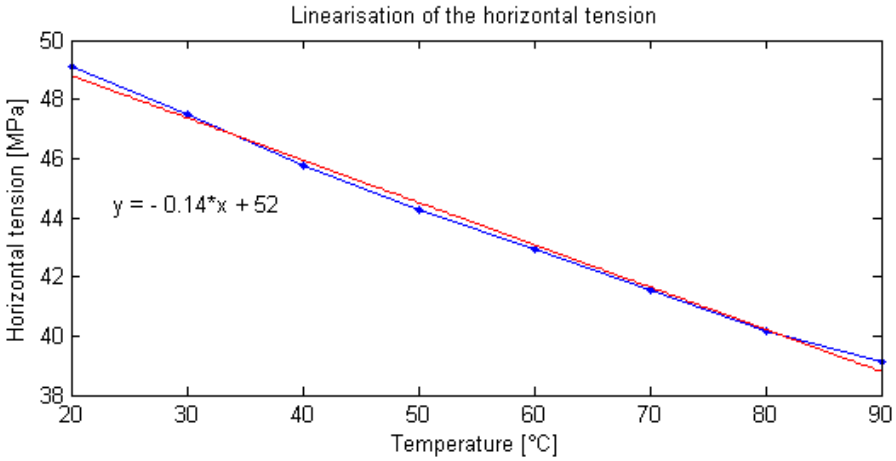

Figure B.7: The plot of data set for section 7

Table B.8 and Figure B.8 represent the section of spans between masts nr.83 to nr.94.

Temperature °C	Tension [MPa]
20	46.23
30	44.50
40	42.87
50	41.12
60	39.50
70	38.17
80	36.81
90	35.43

Table B.8: The data set for section 8

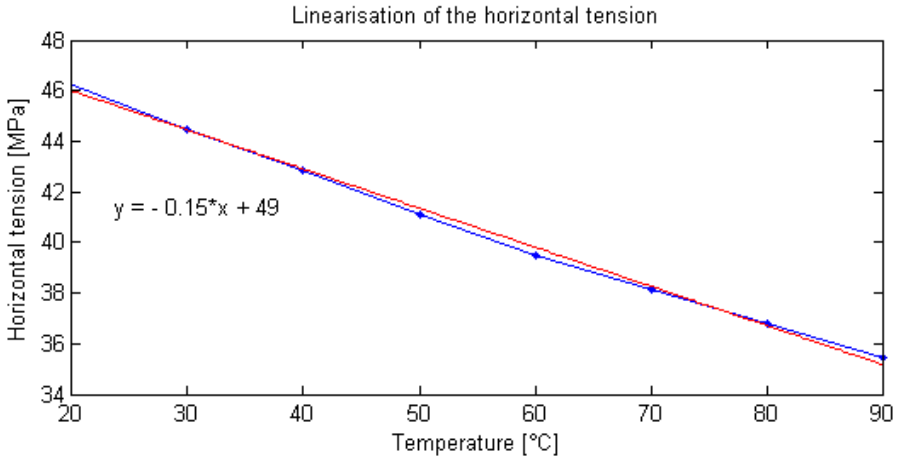

Figure B.8: The plot of data set for section 8

Table B.9 and Figure B.9 represent the section of spans between masts nr.94 to nr.98.

Temperature °C	Tension [MPa]
20	-
30	-
40	-
50	-
60	-
70	30.56
80	28.96
90	27.37

Table B.9: The data set for section 9

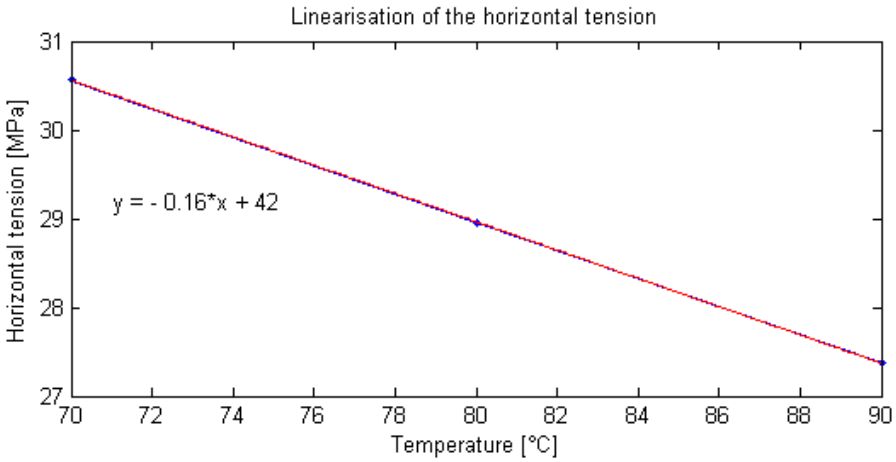

Figure B.9: The plot of data set for section 9

Table B.10 and Figure B.10 represent the section of spans between masts nr.98 to nr.107.

Temperature °C	Tension [MPa]
20	-
30	-
40	-
50	26.42
60	24.73
70	23.28
80	21.69
90	20.03

Table B.10: The data set for section 10

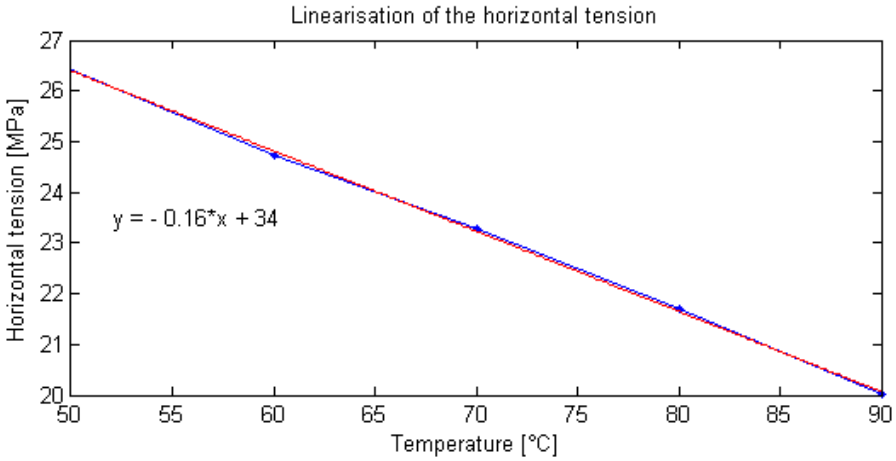

Figure B.10: The plot of data set for section 10

Table B.11 and Figure B.11 represent the section of spans between masts nr.108 to nr.109.

Temperature °C	Tension [MPa]
20	-
30	-
40	-
50	51.00
60	49.88
70	48.42
80	46.67
90	44.82

Table B.11: The data set for section 11

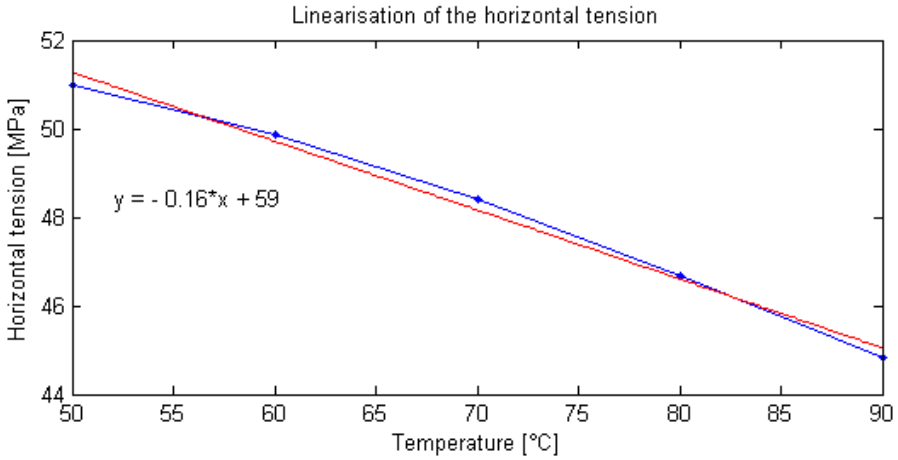

Figure B.11: The plot of data set for section 11

Table B.12 and Figure B.12 represent the section of spans between masts nr.113 to nr.116.

Temperature °C	Tension [MPa]
20	-
30	32.98
40	32.34
50	30.52
60	28.93
70	27.42
80	25.84
90	24.56

Table B.12: The data set for section 12

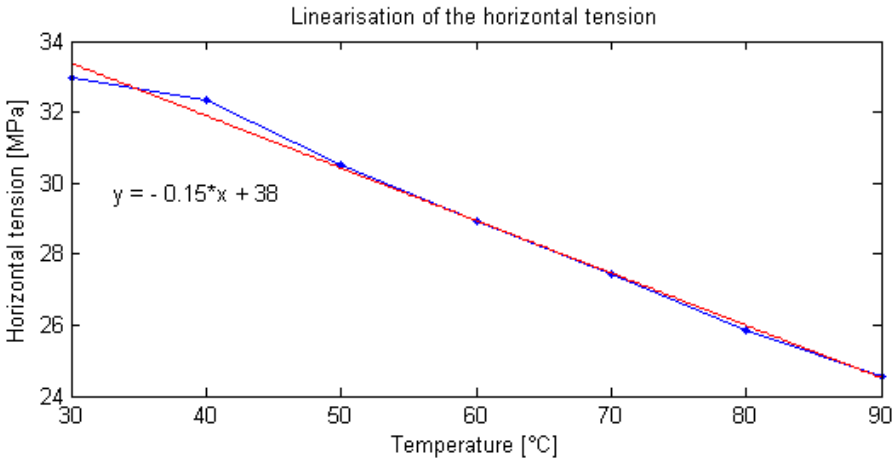

Figure B.12: The plot of data set for section 12

Table B.13 and Figure B.13 represent the section of spans between masts nr.116 to nr.120.

Temperature °C	Tension [MPa]
20	-
30	-
40	49.29
50	48.51
60	46.96
70	45.06
80	43.50
90	41.87

Table B.13: The data set for section 13

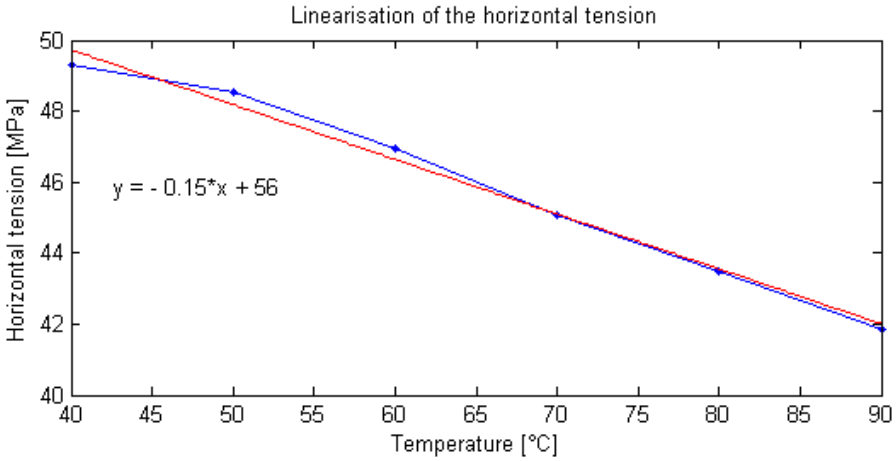

Figure B.13: The plot of data set for section 13

Table B.14 and Figure B.14 represent the section of spans between masts nr.120 to nr.124.

Temperature °C	Tension [MPa]
20	-
30	-
40	34.34
50	34.04
60	32.53
70	30.63
80	29.09
90	27.73

Table B.14: The data set for section 14

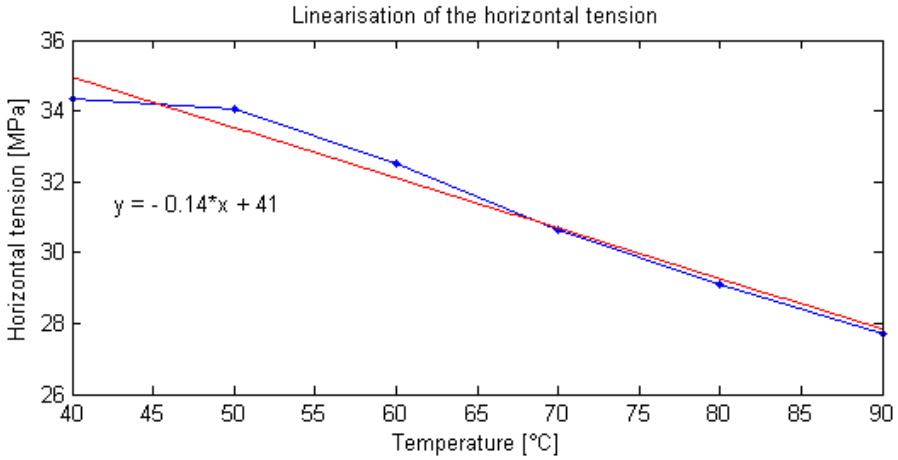

Figure B.14: The plot of data set for section 14

Table B.15 and Figure B.15 represent the section of spans between masts nr.124 to nr.129.

Temperature °C	Tension [MPa]
20	-
30	-
40	-
50	-
60	-
70	-
80	46.36
90	45.08

Table B.15: The data set for section 15

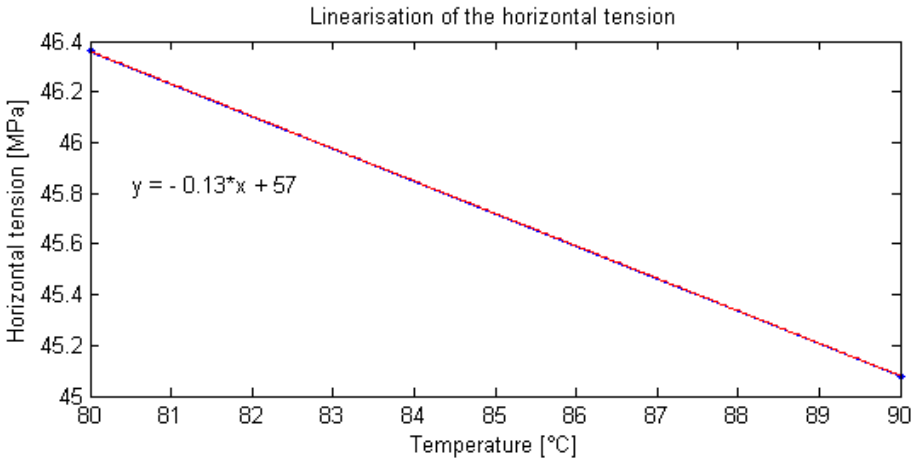

Figure B.15: The plot of data set for section 15

Table B.16 and Figure B.16 represent the section of spans between masts nr.134 to nr.143.

Temperature °C	Tension [MPa]
20	49.15
30	47.60
40	45.76
50	44.08
60	42.53
70	40.92
80	39.49
90	38.31

Table B.16: The data set for section 16

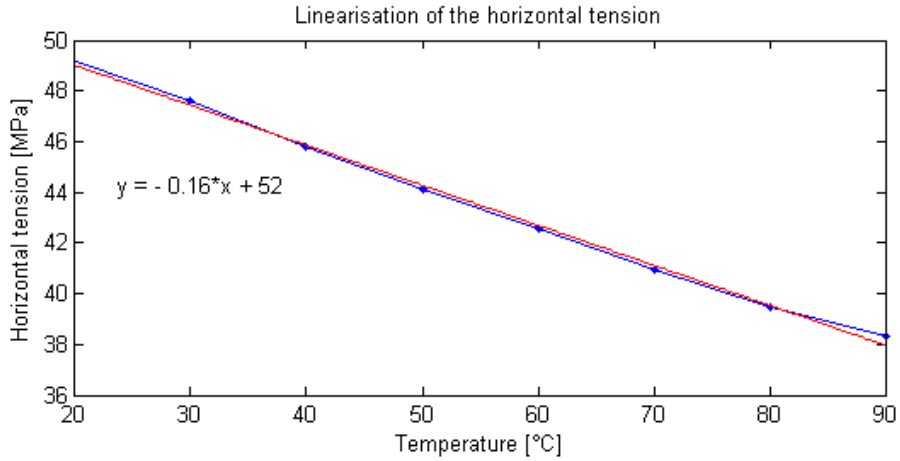

Figure B.16: The plot of data set for section 16

Table B.17 and Figure B.17 represent the section of spans between masts nr.143 to nr.147.

Temperature °C	Tension [MPa]
20	48.54
30	47.24
40	45.42
50	43.78
60	42.13
70	40.41
80	39.04
90	37.77

Table B.17: The data set for section 17

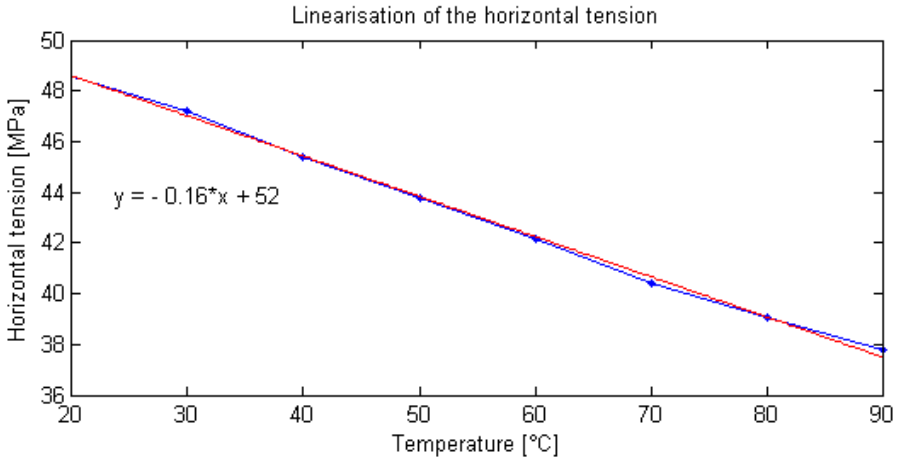

Figure B.17: The plot of data set for section 17

The blanks in the previous tables represent events where there did not exist intersection of the curves for the catenary and the elastic calculations.
For the sections between masts nr.109 and nr. 113, nr.129 and nr.134, nr. 147 and nr. 151, there does not exist measurements for the tension at 5℃. There is there fore not possibility of linearisation of these sections and there fore will there be used average values of the linearisation in these sections.

C Impedance Measurements

In this chapter impedance measurements conducted by Landsnet's emplyees will be introduced.

On 6. April 2013 the impedance of the BR1 connection was measured by using the OMICRON CP CU1 combined with CPC 100 measuring device. The BR1 connection was taken out of service 24 hours before the measurement took place and the estimated conductor temperature was there fore equal to the ambient air temperature, 2℃.
The measurement setup can be seen in Figure C.1.

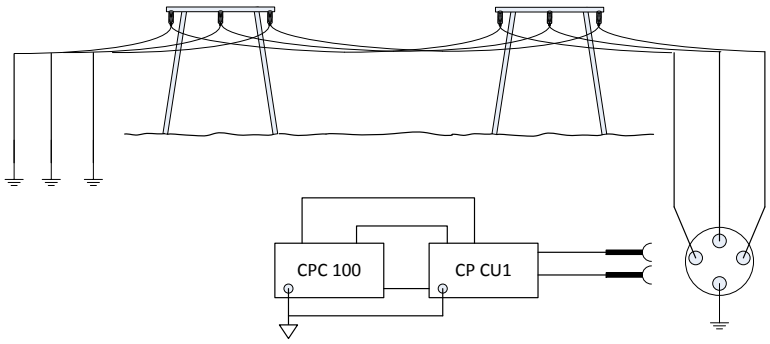

Figure C.1: Setup of the OMICRON CP CU1 and CPC 100.

The far end of the transmission line is grounded and the OMICRON CPC 100 is connected via the CP CU1. A current is injected to the transmission line at 30, 70, 90, 110 and 130 Hz. The current is not injected at 50 Hz in order to avoid possible interference of noise from other substations. The impedance is measured by conducting four measurements. Phase one to phase two(L1-L2), phase two to phase three (L2-L3), phase one to phase three (L1-L3) and three in parallel to ground (L1||L2||L3-E). The impedance at 50 Hz is calculated by computing the average from 30 Hz and 70 Hz measurements. Figure C.2 shows how the impedance increases with increased frequency for the L1-L2 measurement.

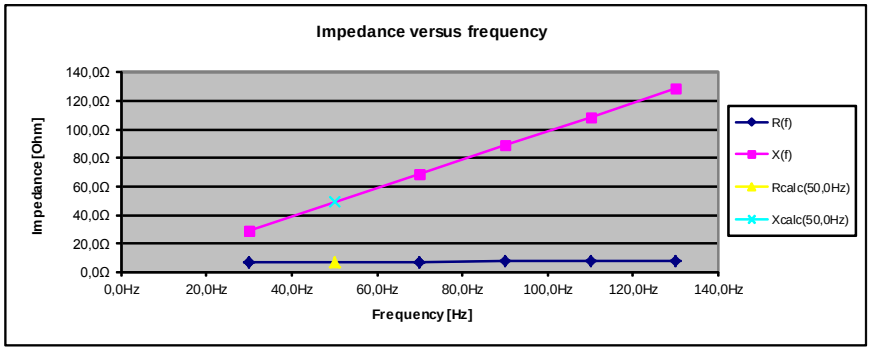

Figure C.2: Impedance calculation at 50 Hz.

This is done for all four measurements and the results from the measurements are in Table C.1.

Measurements	R [Ω]	X [Ω]
L1 - L2	7.974	49.287
L2 - L3	7.967	49.300
L1 - L3	7.990	54.507
L1||L2||L3 - E	4.351	24.228

Table C.1: Results of the impedance measurements

Computing the resulting positive sequence impedance and the zero sequence impedance is done as following equations demonstrates.

$$R_1 = 0.5\frac{(L1-L2)+(L2-L3)+(L1-L3)}{3} = 0.5\cdot\frac{7.974+7.967+7.990}{3} = 3.989\ \Omega$$

$$R_0 = 3(L1||L2||L3-E) = 3\cdot 4.351 = 13.054\ \Omega$$

The same formula is used for the reactance.

Impedance results	R [Ω]	X [Ω]
Positive sequence impedance	3.989	25.516
Zero sequence impedance	13.054	72.685

Table C.2: Results of the impedance measurements

Bibliography

[1] P. Kundur, N.J. Balu, and M.G. Lauby. *Power System Stability and Control*. The Epri Power System Engineering. McGraw-Hill Education, 1994. ISBN 9780070359581.

[2] Landsnet. Various information, february 2013. URL `www.landsnet.is`.

[3] Landsvirkjun. Various information, february 2013. URL `www.landsvirkjun.is`.

[4] Orkuveita Reykjavíkur. Various information, february 2013. URL `www.or.is`.

[5] HS Orka. Various information, february 2013. URL `www.hsorka.is`.

[6] EFLA Consulting engineers. Endurmat á hitaflutningsgetu brennimelslínu 1: 220 kv háspennulína. Technical report, 2009.

[7] FERC. Federal energy regulatory commission, april 2013. URL `www.ferc.gov`.

[8] Jennifer L. Canty, Bill Frischling, and David Frischling. Weatherbase, march 2013. URL `www.weatherbase.com`.

[9] Scheitzer Engineering Laboratories. SEL-487E Data Sheet, 2008.

[10] H. Saadat. *Power System Analysis*. McGraw-Hill series in electrical and computer engineering. McGraw-Hill, 2002. ISBN 9780072848694.

[11] J. Duncan Glover, Mulukatla S. Sarma, and Thomas J. Overbye. *Power System Analysis and Design*. Cengage Learning, fourth edition, 2005.

[12] N. Tleis. *Power Systems Modelling and Fault Analysis: Theory and Practice*. Newnes Power Engineering Series. Elsevier Science, 2007. ISBN 9780080554273.

[13] C.H. Edwards and D.E. Penney. *Calculus: Early Transcendentals*. Pearson Prentice Hall, 2008. ISBN 9780136158400.

[14] Karl Valur Guðmundsson. Virk hitaflutningsmörk háspennulína. Technical report, Reykjavik University School of Science and Engineering, 2011.

[15] W.Z. Black and R.L. Rehberg. Simplified model for steady state and real-time ampacity of overhead conductors. *IEEE Transactions on Power Apparatus and Systems*, PAS-104(10):12, October 1985.

[16] ELSAM. Strømbelastningsevne for luftledninger og leder i friluftsstationer, september 1980.

[17] Y.A. Çengel and R.H. Turner. *Fundamentals of Thermal-Fluid Sciences*. McGraw-Hill Mechanical Engineering. McGraw-Hill, 2008. ISBN 9780071266314.

[18] Murray W. Davis. A new thermal rating approach: The real time thermal rating system fo strategic overhead conductor transmission lines part 2. *IEE Transactions on Power Apparatus and Systems*, PAS-96(3):15, May/June 1977.

[19] L.L. Grigsby. *Electric Power Generation, Transmission, and Distribution*. The Electric Power Engineering Handbook. Taylor & Francis Group, 2012. ISBN 9781439856284.

[20] ÍST EN 50341-1 Overhead elelectric lines exceeding AC 45 kV - Part 1: General requirements - Common specifications.

[21] F. Kiessling, P. Nefzger, U. Kaintzyk, and J.F. Nolasco. *Overhead Power Lines: Planning, Design, Construction*. Power Systems. Springer, 2003. ISBN 9783540002970.

[22] Suparule Systems Limited. *Suparule Cable Height Meter*. URL `www.suparule.com`.

[23] OMICRON. Cp cu1 multi-purpose coupling unit for cpc 100, October 2007. URL `www.omicron.at`.

[24] Verkfræðistofan AFL. Raftæknileg hönnun háspennulína, March 1992.